1976 Institute of Metals Lecture
The Metallurgical Society of AIME

Transformation from Austenite in Alloy Steels

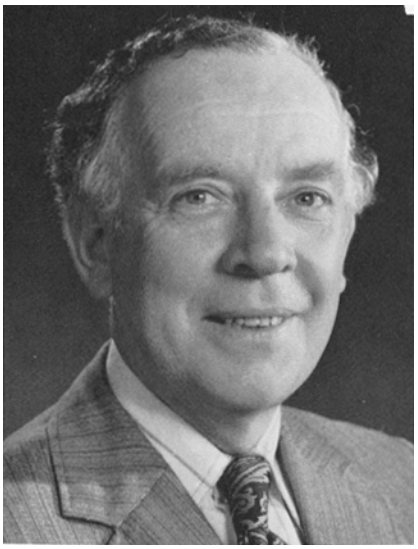

R. W. K. HONEYCOMBE
R. F. Mehl Medalist

This paper is concerned with the direct transformation of austenite at high temperatures to form ferrite and alloy carbide dispersions. The ferrite/austenite interfaces vary from high energy random boundaries to low energy planar boundaries which grow by step propagation, while the alloy carbide morphologies include a pearlitic form, fine fibers and fine banded arrays of particles. It is shown that these morphologies are closely related to the mode of growth of the ferritic matrix. The role of various alloying elements on the carbide dispersion is examined, and the effects of other metallurgical variables on the banded dispersions are discussed, including factors which influence the dispersion stability. The mechanical properties of directly transformed alloy steels are shown to depend largely on the ferrite grain size and the state of the carbide dispersion. Microalloyed steels subjected to controlled rolling provide an excellent example of the achievement of high strength and toughness levels by control of these variables. The paper finally attempts to show how such benefits can be achieved in low and medium alloy steels, and in particular where resistance to creep failure at elevated temperatures is an important property.

THE classical heat treatment for transformable steels has involved quenching from the high temperature austenitic condition to form martensite which, because of its inherently brittle nature, must be subsequently tempered to provide an acceptable compromise between high strength and toughness. It is not the objective of this paper to explain this well trodden path, but to look more closely at the direct transformation of austenite to phases formed at high temperatures, *e.g.* ferrite and ferrite-carbide aggregates which in many cases provide an alternative route to acceptable mechanical properties.

The seeds of this approach to alloy steels were sown by Davenport and Bain in their classical work on the isothermal decomposition of austenite which not only revealed new phases such as bainite, but more importantly demonstrated the effects of alloying elements on the kinetics of the γ/α transformation. One of the most obvious and useful results of their work has been the TTT diagram, now a standard way of de-

The Institute of Metals Lecture was established in 1921, at which time the Institute of Metals Division was the only professional Division within the American Institute of Mining and Metallurgical Engineers. It has been given annually since 1922 by distinguished men from this country and abroad. Beginning in 1973 and thereafter, the person selected to deliver the lecture will be known as the "Institute of Metals Division Lecturer and R. F. Mehl Medalist" for that year

ROBERT HONEYCOMBE holds the Doctor of Science degree from the University of Melbourne as well as the Doctorate of Applied Science (honoris causa) After working several years as a research metallurgist in the Commonwealth Scientific and Industrial Research Organization, he went to the United Kingdom, where he held an ICI Research Fellowship, then the Armourers and Brasiers Fellowship in the Cavendish Laboratory, Cambridge, between 1948 and 1951 In 1951 he joined the Department of Metallurgy at the University of Sheffield as a Senior Lecturer and became Professor of Physical Metallurgy in 1955. In 1966 he was elected to the Goldsmiths Chair of Metallurgy at Cambridge and headship of the Department of Metallurgy and Materials Science which he still holds He is President of Clare Hall, Cambridge, and Honorary Fellow of Trinity Hall, a Vice-President of the Institute of Metallurgists, London, and a Vice-President of the Metals Society.

His research activities started in the cemented carbide and bearing alloy fields, then to a long interest in the deformation of metals and alloys In Sheffield he was infected with what has become a permanent interest in the physical metallurgy of alloy steels but he also likes to work on nonferrous alloys

scribing the kinetics of decomposition of austenite in a vast number of alloy steels. This early work of Davenport and Bain was followed by the elegant investigations of Mehl and colleagues on the nucleation and growth of the important phases pearlite,[1] ferrite, cementite and bainite. These workers not only examined the reaction kinetics, but were also concerned with the morphology and crystallography of the phases, so that our basic understanding of these technologically important transformations was greatly extended.

Since World War II, developments on the one hand in the theory of dislocations and of phase transformations, and on the other, striking experimental advances in electron microscopy, field-ion microscopy and related techniques such as selected area electron diffraction, electron micro-analysis and the atom-probe, have provided the means of delving further into these important problems. Not only has it been possible to describe and explain the kinetics of the reactions in great detail, but also the high resolution microscopic methods have led to a much better understanding of the fine structure of phases already familiar at a much lower limit of resolution, and to methods by which the fine structure can be altered or controlled. The purpose of this lecture is to summarize some of this work carried out within the last decade, and to show its relevance to such areas of technological importance as control-rolled micro-alloyed steels and low alloy steels for use at elevated temperatures.

1. THE AUSTENITE-FERRITE REACTION

From the many observations made on the initiation of the austenite to ferrite reaction, it is clear that at the higher transformation temperatures (above 700°C) nucleation takes place predominantly at the austenite grain boundaries, in common with the formation of many proeutectoid phases in other alloy systems, because the boundaries are both energetically favorable nucleation sites and also provide faster paths for diffusion. C. S. Smith[2] first proposed that the new ferrite nuclei would have one coherent or semicoherent boundary with the austenite, and thus normally a random or incoherent boundary with the adjacent austenite grain. The normal orientation relationship between austenite and ferrite is the Kurdjumov-Sachs relationship (K-S) which applies to Widmanstätten ferrite[3] and indeed probably in many cases to ferrite with an equiaxed appearance, *viz.*

$\{111\}_\gamma \,//\, \{110\}_\alpha$ (habit plane)

$\langle 110\rangle_\gamma \,//\, \langle 111\rangle_\alpha$.

This matching of the closest packed planes in the bcc and fcc lattices gives the lowest degree of atomic misfit. However recent work by Liu *et al*[4] has shown that the habit plane of Widmanstätten ferrite is not exactly $\{111\}_\gamma$ but is scattered 4 to 20 deg about that plane.

In the classification of ferritic morphologies originated by Dubé *et al*[5] and extended in detail by Aaronson,[6] it has been assumed that at the highest transformation temperatures and low supersaturations (800°C and above), the incoherent γ/α boundaries are more mobile leading to growth of allotriomorphs on the appropriate side of the austenite grain boundaries. As the transformation temperature is lowered the tendency for the growth of ferrite in the Widmanstätten mode increases, until it is clear that at high supersaturations the K-S related ferrite is predominant within the former austenite grains. The work of Hillert and colleagues[7] has established this general trend, by carrying out partial transformation at two different temperatures.

From studies of the growth of Widmanstättan ferrite laths or plates, it has been found that the laths increase both in thickness and in length as transformation proceeds. As the plate boundaries (as distinct from the edges) are assumed to be at least semicoherent with the austenite, a mechanism is needed to explain the thickening process.* Aaronson[6] first proposed that thickening occurred by the lateral movement of small ledges or steps along the coherent faces, the steps being short lengths of incoherent boundary (Fig. 1). These ledges have been observed on many allotriomorphs and Widmanstätten-type phases in ferrous and non-ferrous alloys, for example Kinsman and Aaronson[8] have used thermionic emission electron microscopy to study the dynamic growth of ferrite laths, and have been able to measure the velocity of ledge movement. It now appears that this is a very common mode of growth of ferrite in austenite over a wide range of transformation temperature. For example, Fig. 2 shows four stages of transformation in a ternary iron-12 pct Cr-0.2 pct C alloy which has been isothermally transformed at 620–640°C and observed by photo-emission electron microscopy* (which allows observation at much lower temperatures than thermionic emission microscopy). The photographs show the nucleation and growth of several allotriomorphs of ferrite which in all cases have planar interfaces, and in favorable conditions the movement of steps (indicated by the arrow) can be readily observed. It seems clear that, although a single ferrite nucleus can grow only into one adjacent austenite grain with the K-S relationship, its growth into one or

*In this paper no attempt will be made to survey the many kinetic studies on the growth of ferrite, mainly by Aaronson and coworkers. This work has been summarized elsewhere.[8,9]

*These observations were made by Dr. D. V Edmonds and the author at Neuchâtel, Switzerland, by courtesy of Professor W. Form.

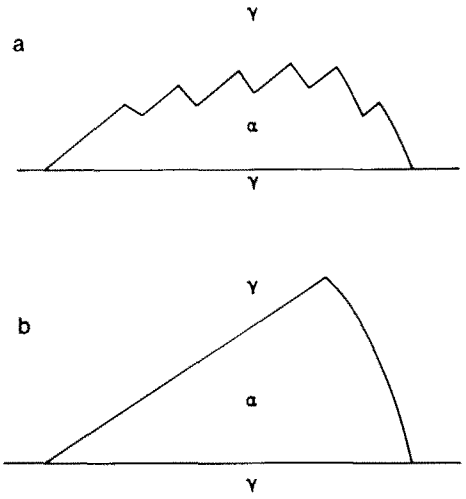

Fig. 1—Growth of ferrite from an austenite grain boundary by step movement. Schematic. (Kinsman and Aaronson)[8]

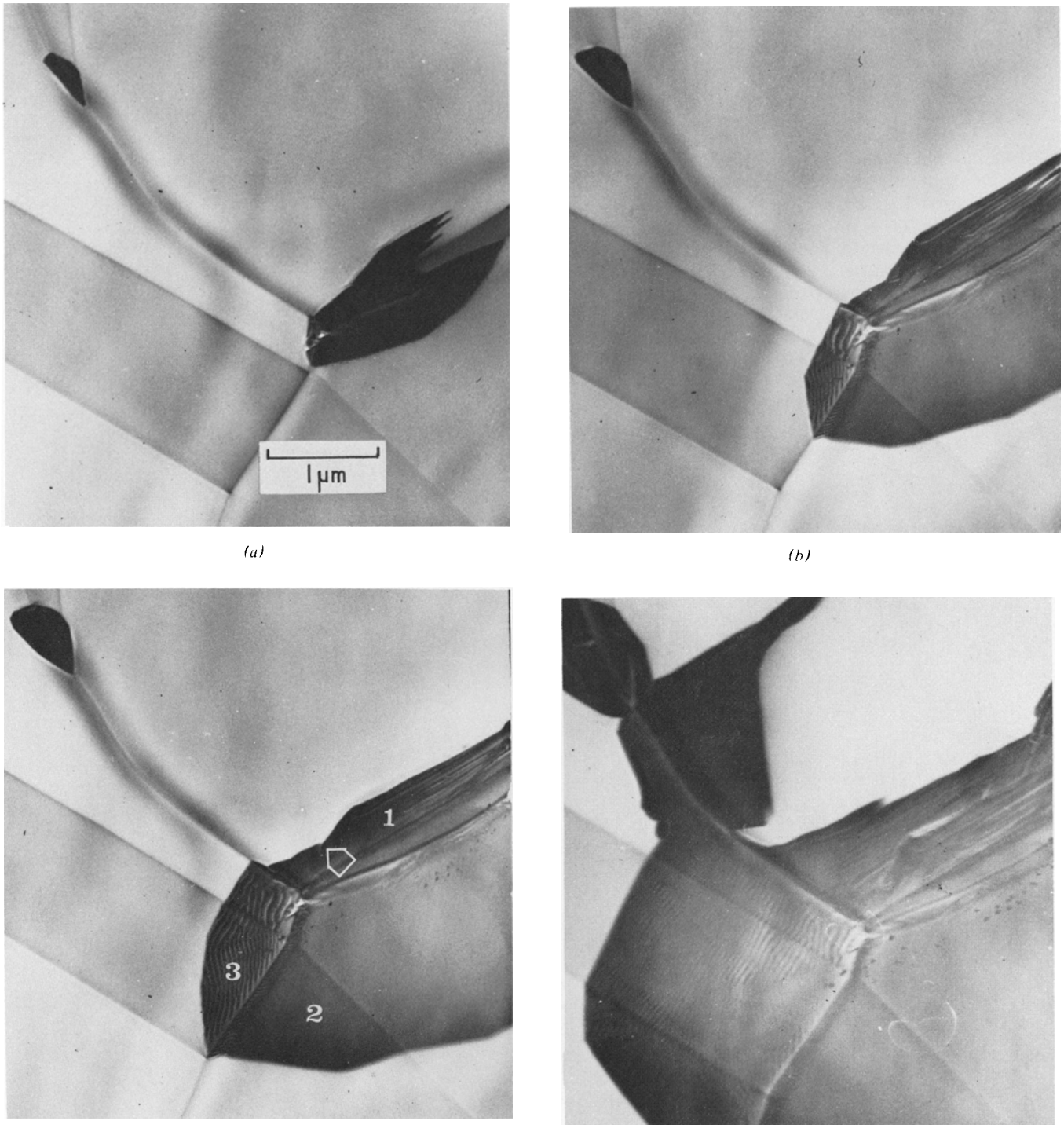

Fig. 2—Four stages in the γ/α transformation in an Fe-12Cr-0.2C alloy transformed at 620–640°C. Photo-emission electron micrographs, magnification 1,840 times. (Edmonds and Honeycombe)

more other grains with which it must have a random relationship, often leads to the development of facetted interfaces rather than curved ones. This is presumably a result of the interface adopting lower energy configurations, and it is interesting to speculate whether these facetted interfaces also grow by the propagation of small steps. The α grain in the center of Fig. 2 is growing into three grains as indicated by regions 1, 2 and 3; one interface in region 1 is clearly growing by step migration, whereas the other two are facetted, however these interfaces could have steps below the limit of resolution (~30 nm). A similar situation appears to prevail in the small ferrite grain at the top of the photograph. One is forced to conclude that migration of truly curved high energy ferrite/austenite boundaries is rare and likely only to occur at higher transformation temperatures. Recent work by Bee[10] on binary iron-chromium alloys confirms this view, in so far as ferrite formed between 550 and 750°C gave frequent evidence of growth steps

(Fig. 3(*a*)), while ferrite formed at 800°C had curved boundaries with the austenite (Fig. 3(*b*)).

2. THE PEARLITE REACTION

The pearlite reaction has received a great deal of study, as befits a structure which is one of the most familiar in commercial steels, yet there are still numerous problems which have received insufficient attention, in particular the modification of the structure by the addition of alloying elements. Like ferrite, pearlite is preferentially nucleated at austenite grain boundaries, but when these are already the sites for prior formation of proeutectoid ferrite or cementite, the pearlite nodules grow from the interfaces of these two phases with austenite. It has recently been shown[11] that the two main ferrite/cementite orientation relationships in pearlite depend on whether the pearlite nucleates at a "clean" austenite boundary or on a proeutectoid phase.

Thin foil electron microscopy has thrown some light on the vexed questions of nucleation and growth of pearlite. It now seems clear that either cementite or ferrite can nucleate pearlite nodules, and the long de-

(*a*)

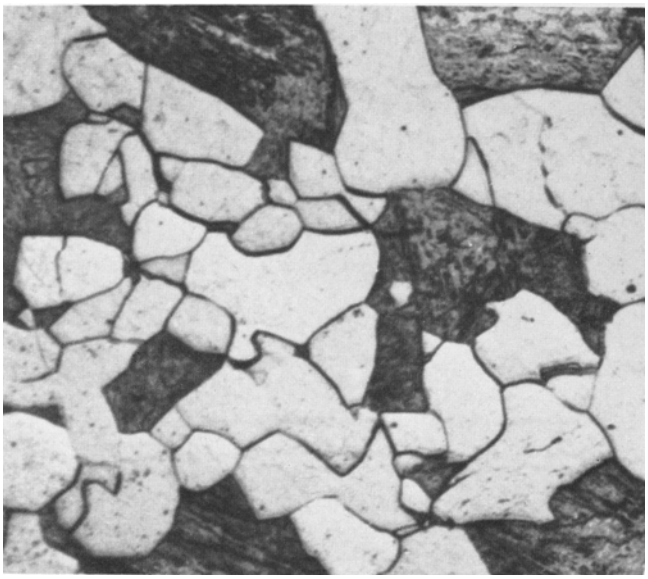

(*b*)

Fig. 3—Transformation in an Fe-10Cr alloy. (*a*) 30 s at 750°C, magnification 700 times. (*b*) 5 min at 800°C, magnification 300 times. Optical micrographs. (Bee)[10]

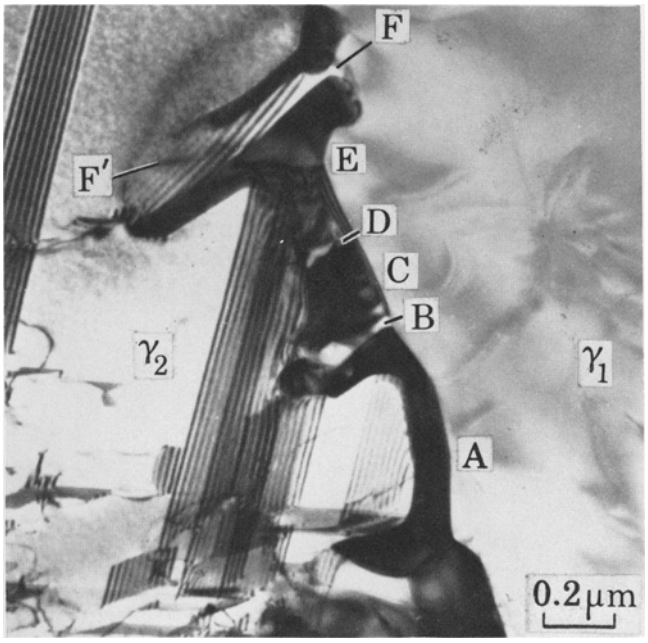

(*a*)

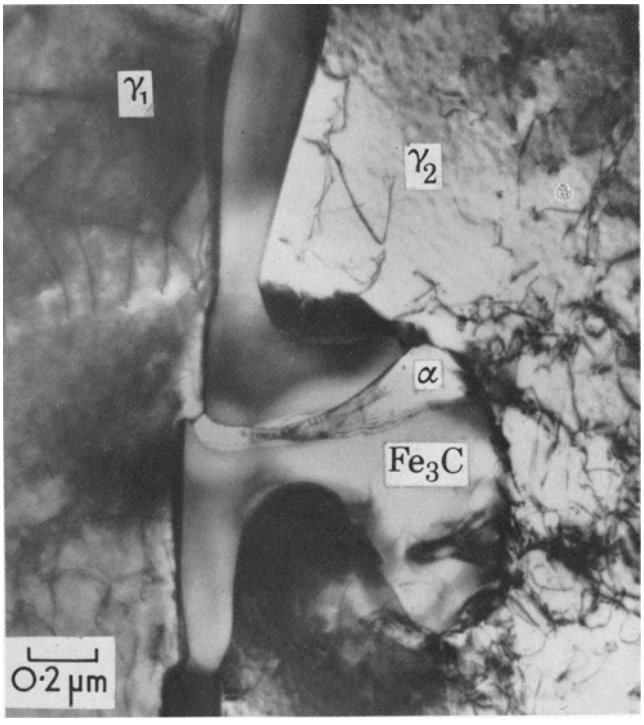

(*b*)

Fig. 4—The nucleation of pearlite at grain boundaries of austenite in an Fe-12 pct Mn-0.8 pct C steel. (*a*) Side-by-side nucleation of Fe_3C and α-iron. Cementite: *A*, *C*, *E*; ferrite: *B* and *D*; austenite: *FF′*. (*b*) Branching of the Fe_3C and α-iron in a nucleus—note the continuity of Fe_3C with the grain boundary carbide. Thin foil E.M. (Dippenaar and Honeycombe)[11]

bated question of sympathetic sideways nucleation has been confirmed in thin foils[11] (Fig. 4(*a*)). At an early stage of growth of a nucleus, dark field electron microscopy can readily identify the small laths of ferrite and cementite, as well as the untransformed austenite, if a steel of suitable composition is chosen for investigation. Happily the alternative explanation of the development of the lamellar structure, namely branching of the ferrite and cementite laths, has also been shown to take place (Fig. 4(*b*)). So once again a controversy, hotly argued in its day, has come to the point where both views are shown to have substance and relevance to the early growth of pearlite nodules.

The addition of alloying elements, particularly strong carbide formers, has a marked effect on the pearlite reaction. In the first place, cementite can take alloying elements into solid solution, *e.g.*, up to 20 wt pct chromium (Entin)[12] in a steel with 3.5 pct Cr 0.4 pct C, but the cementite can then be entirely replaced by an alloy carbide as the alloy content is increased. Mannerkoski[13] observed coarse pearlitic structures in a 14 pct Cr 0.3 pct C steel after transformation in the range 600–800°C, while Campbell[14] found that when a 5 pct Cr 0.2 pct C steel was transformed in the range 700–750°C a coarse pearlitic structure was obtained in which the carbide phase was Cr_7C_3, in agreement with the work of Bungardt *et al*[15] on the iron-chromium-carbon equilibrium diagram. As the chromium content of the steel is increased to 10–12 pct, a coarse pearlitic phase is still obtained at 750°C, but the carbide is now $Cr_{23}C_6$. The morphology is coarse, lath-like and branched (Fig. 5) resembling at least superficially the more familiar pearlitic cementite. While such alloy carbide structures are interesting in the academic sense, they are unlikely to provide mechanical properties in steels which would differ appreciably from normal pearlitic structures, because they have interlamellar spacings between 100 and 500 nm only marginally smaller than fine pearlite. Moreover the high concentration of alloying element needed to produce them cannot be justified on economic grounds.

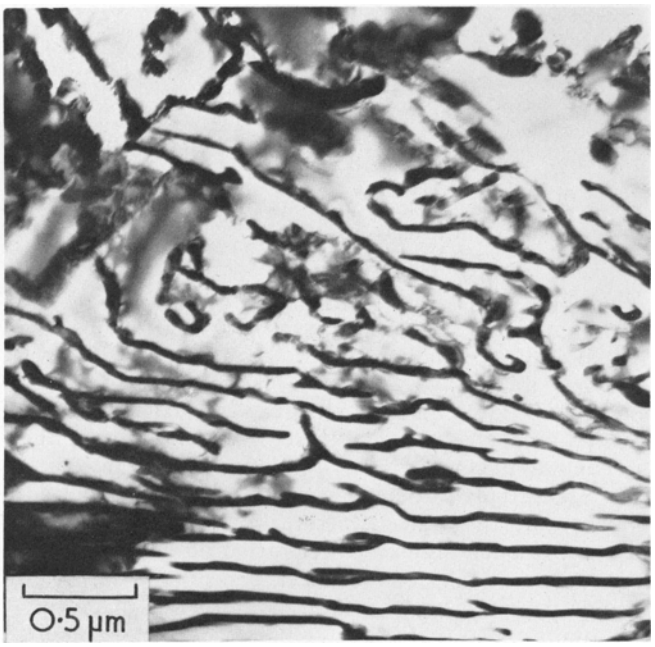

Fig. 5—An Fe-10Cr-0.4 pct C steel transformed 10 min, at 750°C. Thin foil E.M. (Bee)[10]

In many isothermally transformed alloy steels, a much finer directionally grown alloy carbide phase is encountered. The carbide is then in fibrous form, *i.e.* with a more or less equiaxed cross section, and typically the diameter of the fibers is 25 to 50 nm. Such fibers occur in chromium steels in the transformation range 650–800°C. However this morphology is best shown in isothermally transformed molybdenum steels,[16] where Mo_2C forms fine fibers in association with ferrite. The overall morphology of these fine fibrous aggregates is quite complex and variable.[16,17] Some are nodular and have a general similarity with pearlite nodules while others grow straight from austenite grain boundaries with roughly planar boundaries (Fig. 6(*a*)), although no steps are observed in these interfaces between the aggregate and austenite. In other cases the fibers grow in fir-tree configurations, normally from central spines (or sub-boundaries) which have grown out from an austenite grain boundary (Fig. 6(*b*)). As these structures are at least an order of magnitude finer than normal pearlitic structures, and moreover as 0.2 pct carbon provides a "fully eutectoid" structure, they can be used to achieve good mechanical properties. For example, an 0.2 pct carbon steel with 4 pct molybdenum gives a yield stress approaching 50 tsi (770 MNm^{-2}) on transformation in the range 600–650°C.[17] The fibrous carbide morphology which has been found in numerous alloy steels, has been shown to arise primarily during direct isothermal treatment or during controlled cooling of austenite. The carbides shown to exist in this form include Mo_2C, W_2C, VC, Cr_7C_3 and TiC, but the exact circumstances leading to the occurrence of fibrous carbide growth in the face of competing morphologies have yet to be fully understood.

3. INTERPHASE PRECIPITATION

In recent years it has been shown that isothermally transformed alloy steels often possess microstructures which are midway between the two classical eutectoid structures *i.e.* proeutectoid ferrite and pearlite. The microstructure at low resolutions appears to be completely ferritic, and indeed the morphology of the ferrite as revealed in the early stages of transformation is identical with that of proeutectoid ferrite (Fig. 7(*a*)). However high resolution electron microscopy reveals very fine banded dispersions of alloy carbides within the ferrite (Fig. 7(*b*)), which is usually referred to as interphase precipitation.[18] The composition of the carbide phase depends on the composition of the steel, but almost all the familiar alloy carbides adopt this morphology after appropriate heat treatments, including VC,[18] CbC,[19] TiC,[20] Mo_2C,[16] Cr_7C_3,[13,14] $Cr_{23}C_6$,[13,14] W_2C,[21] M_6C.[22] The fine state of the dispersions contrasts with the much coarser pearlite morphology referred to above. It is thus clear that this type of reaction provides a major way of strengthening of ferrite which deserves detailed consideration, as it is a *direct* route in contrast to the classical quench and temper approach to dispersion strengthened ferrite.

It therefore seems appropriate at this stage to sum-

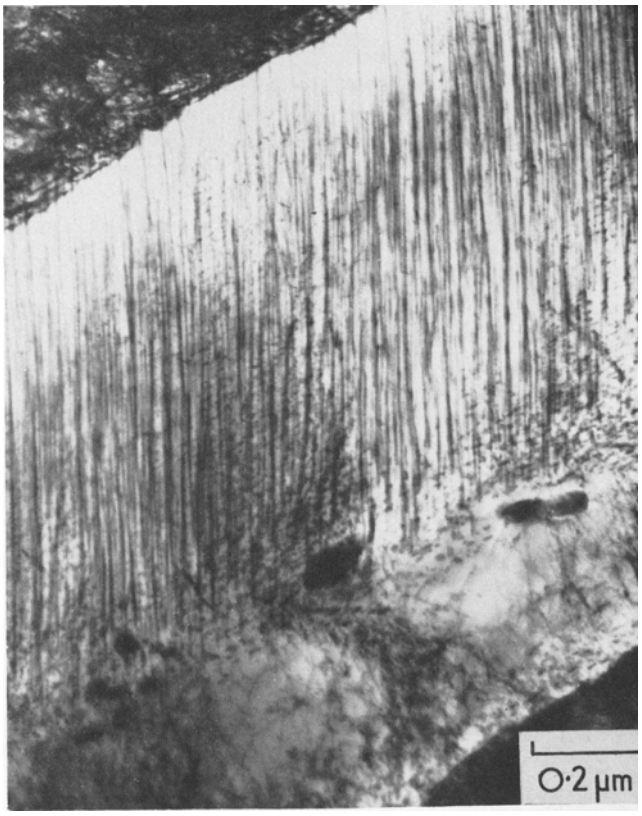

(a)

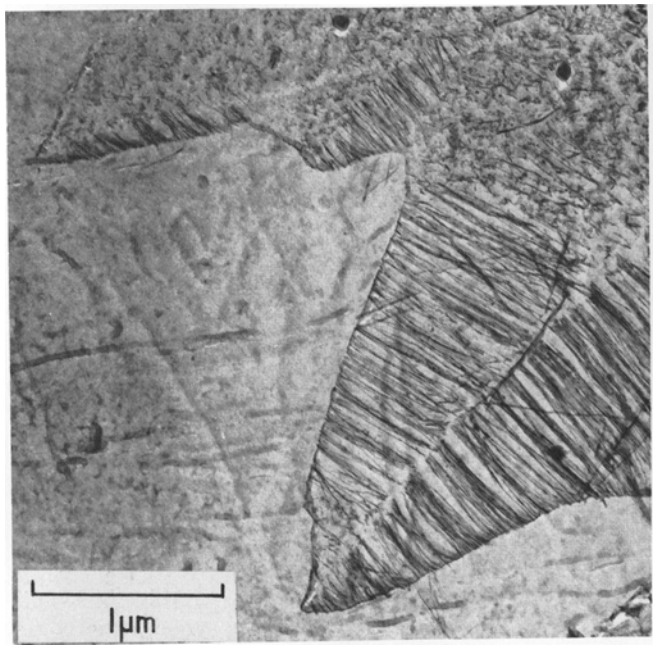

(b)

Fig. 6—(a) Fe-4Mo-0.2C transformed 20 min at 650°C. Thin foil EM, magnification 70,000 times. (Berry)[16]. (b) Fe-4Mo-0.2C transformed 2 h at 650°C, magnification 25,000 times. (Edmonds)[17]

marize our knowledge concerning this type of precipitation phenomenon.

3.1 Early Observations

It has been known for a long time that commercial steels grain-refined with columbium (niobium) and/or vanadium reach greater strength levels after controlled rolling than expected by the ferrite grain size achieved, using the Hall-Petch analysis for the dependence of yield stress on grain size. It was realized that the increased strengthening must arise from alloy carbide precipitation,[23] and indeed fine particles of CbC often aligned in rows were detected in as-rolled and normalized grain refined mild steels, and found to be usual in such steels.[24-26] Detailed electron microscopy investigations[19-21] have shown that the fine carbide precipitates are often much less than 10 nm in diameter, and that they are normally arranged in bands, the spacing of which may be as small as 5 nm, but can vary up to 50 nm.

(a)

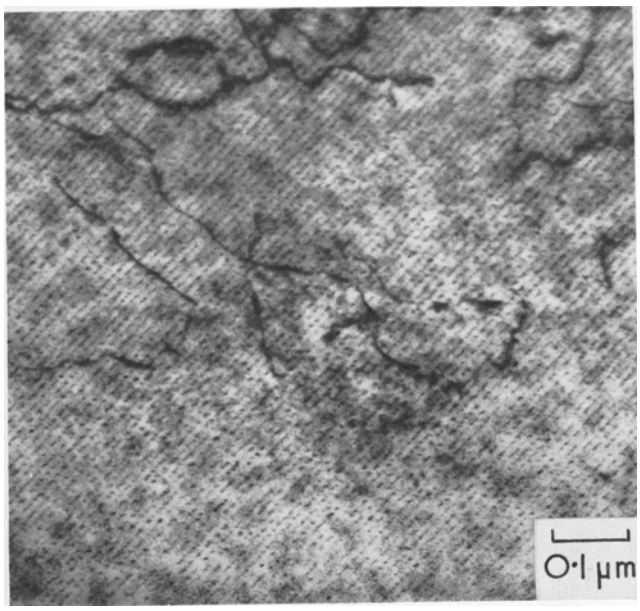

(b)

Fig. 7—Fe-0.75 pct V-0.15 pct C. (a) 10 s at 680°C. Optical micrograph, magnification 125 times. (b) 5 min at 725°C. Thin foil EM. (Batte and Honeycombe)[29]

One view advanced for the apparently linear precipitate arrays was that they were nucleated on dislocations in the ferrite or in the austenite;[27,28] however, while such imperfections do nucleate alloy carbide particles, they do not normally result in regular precipitate arrays. The alternative hypothesis[18,19] which has now gained strong support because of decisive structural evidence, is that the carbide particles are nucleated periodically at the γ/α interfaces, as they move through the austenitic grains.

We shall examine the phenomenon in greater detail below, in an attempt to outline the factors which determine whether the interphase morphology is adopted, or whether the carbides grow in a fibrous fashion or on dislocations, which appear to be the three main competing morphologies. However, it should be pointed out that in some steels, *e.g.* Cr steels, the alloy pearlitic structure is also in competition with the above morphologies, with the result that the observed microstructures are frequently complex. Fortunately there are other alloy steels, *e.g.* those based on vanadium and on titanium in which the structures are less complex, and can be more readily analyzed. Chromium steels however possess one advantage, in so far as the chromium carbide precipitates and the interband spacings are frequently quite coarse, so that the growth of individual particles can be studied.

3.2 Quantitative Metallographic Observations

Batte and the author[29] have investigated the isothermal transformation of several high purity vanadium steels in the temperature range 700–850°C, keeping the vanadium-carbon ratio constant (5 : 1), but varying the volume fraction of vanadium carbide precipitate from 0.23 to 1.23 pct. After transformation all the steels showed ferritic structures with predominantly interphase precipitation of vanadium carbide. The precipitate parameters, *viz.* the band spacing and the particle size were found to vary systematically with transformation temperature (Fig. 8), increasing with temperature and with decreasing supersaturation. It will be noted that precipitate band spacings of around 10 nm were observed after transformation at 725°C the lowest temperature at which measurements were made. However the same reaction occurs at least down to 650°C at which point it begins to compete with the upper bainite reaction, so that spacings much lower than 10 nm are easily achieved, but less readily measured.

There are several other ways in which the dispersion can be varied. Firstly the austenitizing temperature can be changed; in the above experiments high temperatures (1150–1200°C) were used to ensure full solution of vanadium carbide in the austenite prior to transformation. If lower temperatures are used, the amount of vanadium carbide in solution decreases, consequently on transformation the effect is the same as lowering the vanadium and carbon levels, namely the volume fraction of precipitate formed during the γ/α transformation is less, so the band spacing and particle size of the vanadium carbide increases.

A further control of the reaction is by the use of additional alloying elements which either depress the TTT curve and displace it to longer times, or raise the curve and displace it to shorter times. Manganese,

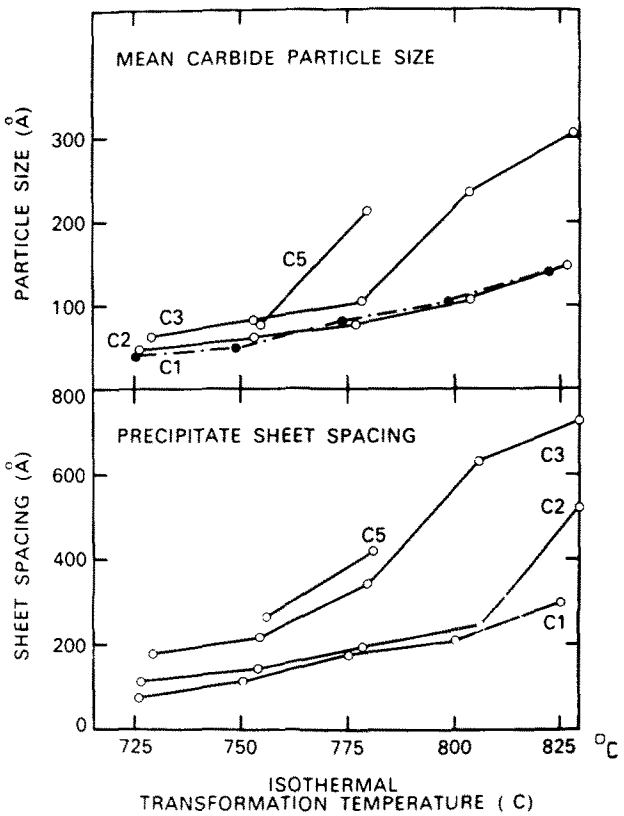

Fig. 8—Isothermal transformation of vanadium steels: dispersion parameters

				Vol. Fract. Precipitate
C1	1.04V	0.20C	0.02Cb	1.23
C2	0.75V	0.15C	0.02Cb	0.93
C3	0.48V	0.09C	0.02Cb	0.55
C5	0.55V	0.04C	0.02Cb	0.23 (Batte and Honeycombe)[29]

chromium and nickel have the first effect, with the result that for a given transformation temperature the dispersion becomes coarser, because the reaction being slower, allows more time for diffusion to occur. However the whole curve is depressed, so that the interphase precipitation reaction can take place at lower temperatures. On the other hand, elements such as silicon and aluminum have been shown to accelerate the basic ferrite reaction; recent unpublished work by Wilyman indicates that these elements accelerate the interphase reaction in Fe-V-C alloys presumably with a refinement of the structure, which it has not yet been possible to measure.

3.3 Mechanism of the Reaction

There is clear evidence that the carbide particles are nucleated at the γ/α boundaries during transformation.

1) Bands are parallel to the γ/α boundaries.[21] This can be observed in favorable circumstances in the early stages of transformation, and the bands follow the changes in direction of the boundary as in Fig. 9, a 4 pct molybdenum steel transformed at 850°C.

2) The direct observation of the interface in chromium steels has shown that the carbide particles nucleate on the interface.[30]

3) The carbide particles are frequently only in one variant of a Widmanstätten relationship.[21,31] This can

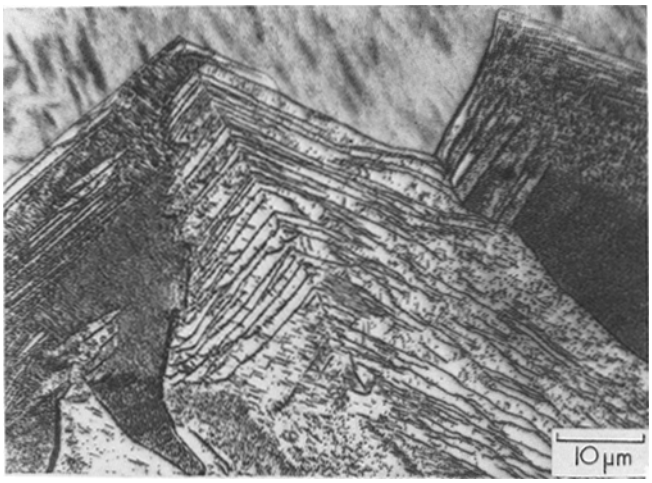

Fig. 9—Fe-4Mo-0.2C transformed 10 min at 850°C. Optical micrograph. (Barbacki)[35]

easily be shown by precipitate dark field electron microscopy. In the case of vanadium carbide, the particles are platelets which often lie on the $\{100\}_{\text{ferrite}}$ plane most nearly parallel to the interface.

4) The orientation relationship of the carbides with the ferrite matrix are the same as those encountered in tempered martensites (except for the limitation of variants referred to in 3). For example the relationship for vanadium carbide in isothermally transformed steels is the same as that found by Baker and Nutting in tempered vanadium steels[32]

$$\{100\}_{VC} \,//\, \{100\}_{\alpha}$$
$$\langle 110\rangle_{VC} \,//\, \langle 100\rangle_{\alpha}\,.$$

Similarly the Mo_2C particles, which are normally rodlets, have the same orientation relationship to ferrite as in tempered Mo steels,[16] *viz*:

$$(011)_{\alpha} \,//\, (0001)_{Mo_2C}$$
$$(100)_{\alpha} \,//\, (2\bar{1}\bar{1}0)_{Mo_2C}$$
$$[100]_{\alpha} \,//\, [2\bar{1}\bar{1}0]_{Mo_2C} \text{ (growth direction)}$$

This crystallographic information taken in conjunction with 1)–3) above indicates that the bands of precipitate *nucleate* at the γ/α interface and *grow* in the α phase. It is not possible to examine the precipitation process at the γ/α interface without giving consideration to the mechanism by which the ferrite phase grows at the expense of the austenite. Examination of a range of steels based on vanadium, titanium, tungsten and chromium has led to the conclusion that in most cases over much of the transformation range, excluding perhaps the highest transformation temperatures, the ferrite interfaces associated with interphase precipitation grow predominantly, but not exclusively by ledge migration. This mechanism is now well established for the growth of "pure ferrite" in the absence of precipitate, as a result of the work of Aaronson and coworkers.[8,9] It is thus interesting to see how the two phenomena of ledge migration and interphase precipitation complement each other in many alloy steels. The observations at temperature in the thermionic emission microscope (Fig. 2) were carried out on such an alloy, in which it was possible occasionally to see interface nucleated bands of precipitate, in addition to the ledges on the ferrite/austenite interfaces, but the resolution of the method did not allow precise observation on the precipitate particles.

To obtain more significant results on the relationship between the ledges and the precipitate,[30,31] it is necessary to use thin foil electron microscopy on steels which have substantial ledges on the interface. One of the best steels is a simple binary alloy Fe-12Cr-0.2C, which on isothermal transformation at 650–750°C provides ledges about 50–400 nm in height. Fig. 10(*a*) and (*b*) shows the same stepped region of the interface in bright field and in precipitate dark field: in the latter photograph the white regions correspond to identically oriented precipitate particles. It can be readily seen that nucleation has occurred along the planar boundary (or "tread") while the ledge itself (or "riser") is free from precipitate. This is an interesting reversal of normal nucleation behavior. Campbell found the boundary plane to correspond to $\{110\}_{\alpha}$, so the boundary was probably of low energy, and thus its mobility would be severely limited, consequently growth of the ferrite occurs by rapid movement of a series of incoherent high energy steps. Normally such sites would be energetically favorable for nucleation of precipitates, but the ledges are *too* mobile for nucleation to occur there. Consequently nucleation takes place on the lower energy, less mobile planar faces as they are extending due to ledge migration. In Fig. 9(*b*) the size of the carbide particles *decreases* as each ledge is approached

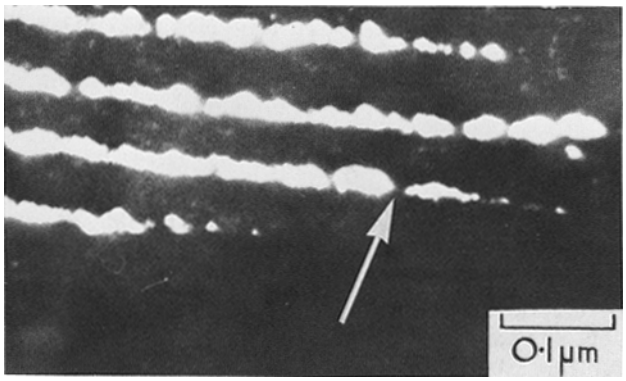

(*a*)

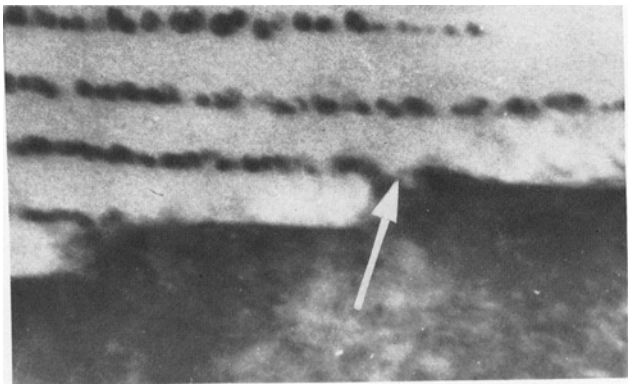

(*b*)

Fig. 10—Fe-12Cr-0.2C transformed 30 min at 650°C; precipitation of $Cr_{23}C_6$. Same area (*a*) bright field, (*b*) dark field. Thin foil EM, magnification 150,000 times. (Campbell)[14]

clearly indicating the sequence of nucleation which was detected in the chromium steel.

Sometimes the movement of a large step is followed by several much smaller steps, which leads to several closely spaced bands of precipitate followed by a large space to the next band of precipitate as a coarser step moves along the interface. The two situations are shown schematically in Fig. 11(*a*) and (*b*) where the latter case gives rise to groups of precipitate bands. These should be distinguished from the more random arrays of particles obtained when a thin foil specimen is tilted so that the bands are at an angle to the foil surface of substantially less than 90 deg.[21] However this tilting experiment is important, as it also shows clearly that the precipitates are not linear but lie in bands or sheets.

There is an alternative way in which the ferrite can grow away from the carbide particles nucleating at the γ/α interface, which appears to occur particularly at high temperatures, and probably when precipitation takes place on a boundary which is of higher energy. It is thus able to move more readily than coherent or semicoherent boundaries. Break away of the boundary from the particles then appears to occur by means of a bowing out mechanism which could occur at various points along a precipitate front.[33] It would be expected that such a bowing out mechanism would lead to some irregular bands of particles, as there would be no need to commence with a planar γ/α boundary, nor would the new boundary after break away be planar. Fig. 12 shows a typical example of an irregular γ/α front in a 12 pct Cr-0.2 pct C steel isothermally transformed at 625°C.

One intriguing observation which has not yet been fully explained is that fine twins are often observed in the ferrite, particularly in steels containing vanadium.[31,34]

4. COMPETITIVE CARBIDE MORPHOLOGIES

In many steels two or three different alloy carbide morphologies frequently exist side by side in association with ferrite, even within a single original austenite grain. The evidence suggests that the fine fibrous carbide ferrite aggregates normally form random high energy boundaries with the austenite, consequently it would be expected that, as in the case

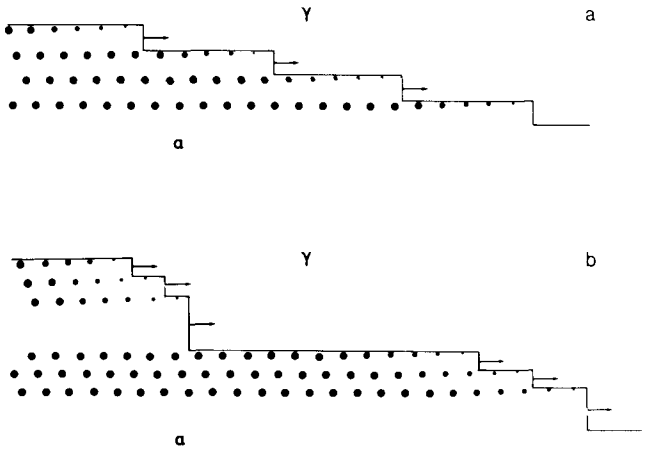

Fig. 11—Mechanism of nucleation and growth of carbides on the γ/α interface. Schematic.

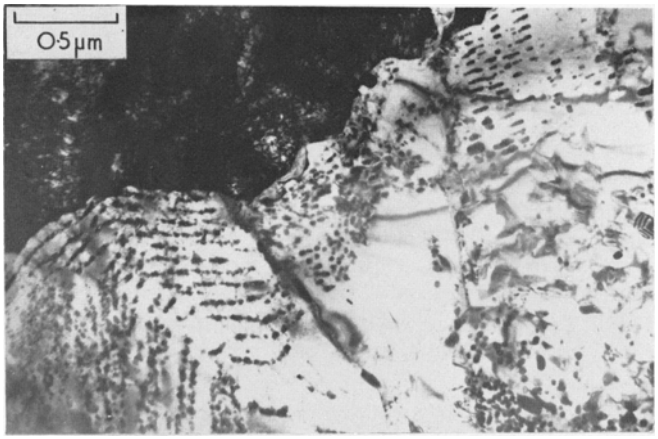

Fig. 12—Fe-12Cr-0.2C transformed 60 min at 625°C. Thin foil EM. (Campbell)[14]

of pearlite, the ferrite and carbide would be unrelated to the austenite into which they were growing. In contrast the interphase reaction is predominantly associated with the movement of high energy steps on low energy, planar boundaries; in this case it would normally be expected that the ferrite would be related by the *K-S* relation to the austenite in which it grows. However, experimental evidence suggests that these are only broad guidelines, and indeed along the same γ/α boundary the morphology can change abruptly (Fig. 13), although the ferrite orientation is unaltered.

Earlier work on the pearlitic and bainitic reactions[7] utilized partial transformation at one temperature followed by further transformation at a lower temperature to elucidate basic features of the two structures. A similar technique has now been applied to alloy carbide precipitation using electron microscopy and electron diffraction to determine orientation changes in ferrite and carbide phases.[35] Working with a steel containing 4 pct molybdenum and 0.2 pct carbon (Fig. 14) it was found that a change in trans-

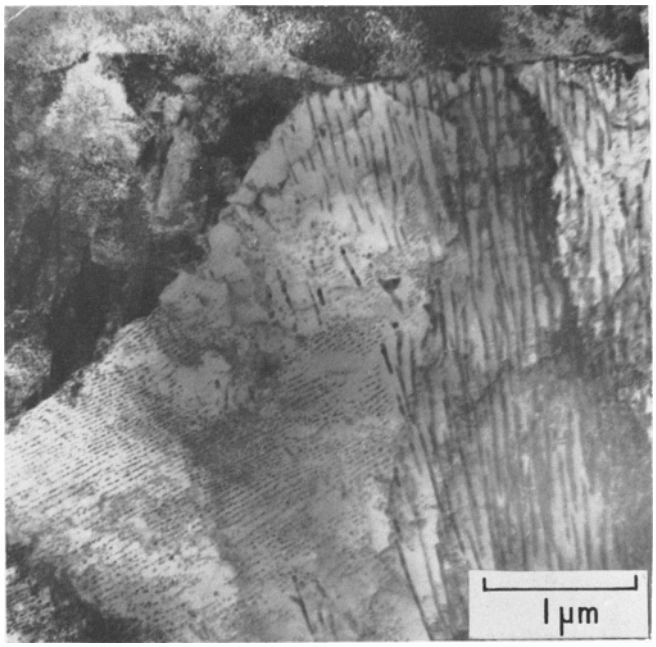

Fig. 13—Fe-5Cr-0.2C transformed 30 min at 650°C. Transition in carbide morphology as the boundary changes orientation. Thin foil EM. (Campbell)[14]

formation temperature from 850 to 725°C had a substantial effect on the carbide dispersion. Fig. 15 shows the transition zone between Mo_2C fibers typical of 850° and 750°C; the orientation remains the same but the spacing has changed by approximately an order of magnitude. Interphase precipitation was more prevalent at 850°C than the fibrous carbide, but on cooling to 725°C (Fig. 14) fibrous Mo_2C growth predominated, and in doing so, stepped ferrite boundaries (arrowed) were replaced by more curved high energy interfaces (Fig. 16). This is perhaps a surprising result, as such morphologies would be expected at higher transformation temperatures. Thus it seems that the fibrous reaction is not completely analagous to the pearlite reaction; the true alloy pearlite reaction appears to be the reaction described in Section 2. Thin foil electron microscopy provided more precise information about the transition, in so far as the orientation of the ferrite was shown to be identical in the two regions, but by using a dark field technique, it was shown that the Mo_2C precipitate assumed a different orientation in the two temperature regimes.

Consequently we have a situation where the orientation of the ferrite matrix is unaffected by a temperature change (either up or down), but the same change

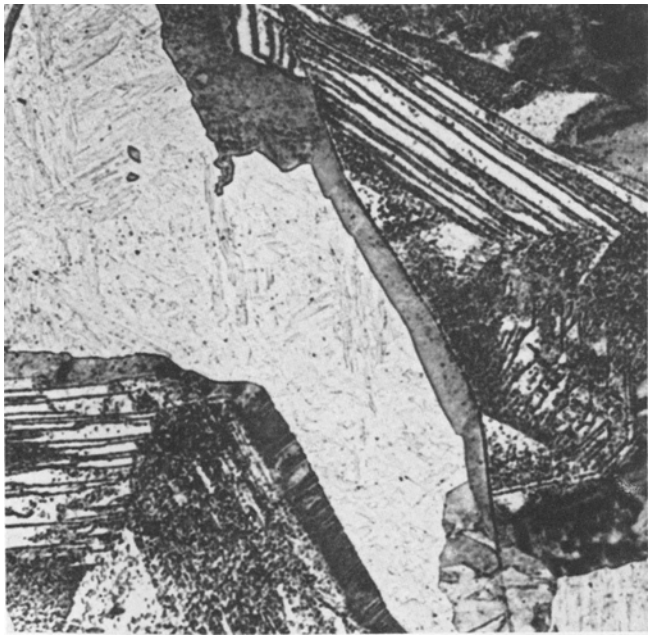

Fig. 14—Fe-4Mo-0.2C. Partial transformation at 850°C followed by further transformation at 725°C. Change from interphase precipitation to fibrous carbide. Optical micrograph, magnification 600 times. (Barbacki)[35]

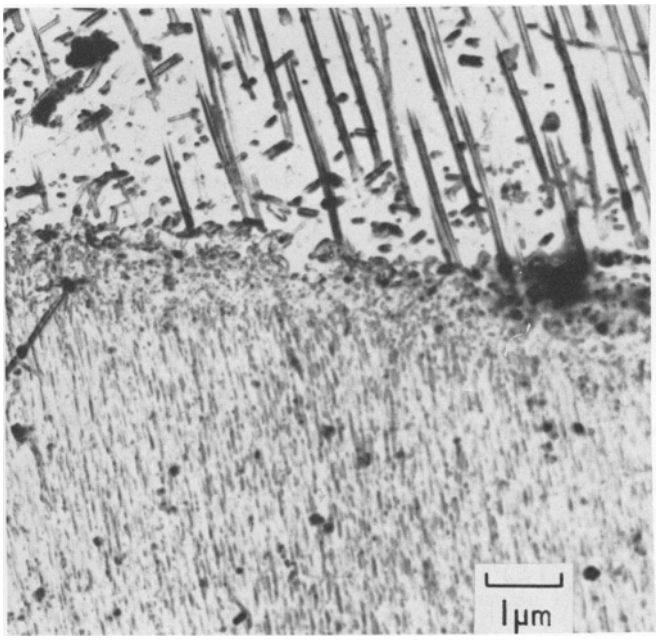

Fig. 15—Fe-4Mo-0.2C. Transformation at 850°C then 750°C. Transition from coarse to fine fibrous Mo_2C. Extraction replica EM. Magnification 10,000 times. (Barbacki)[35]

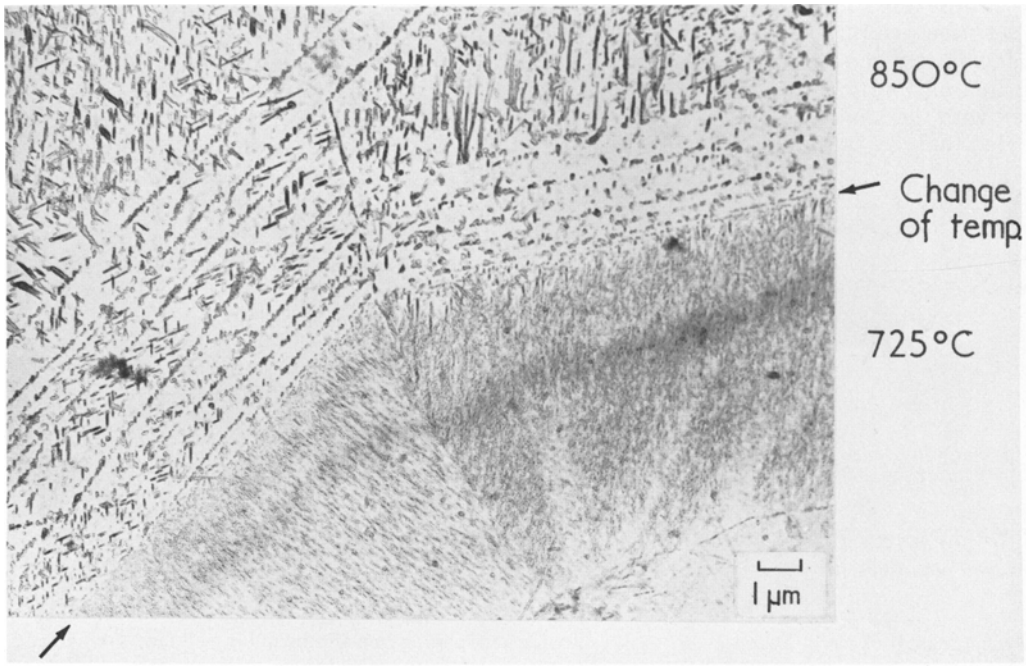

Fig. 16—Fe-4Mo-0.2C. Partial transformation at 850°C followed by further transformation at 725°C. Transition from interphase to fibrous carbide. Extraction replica EM. (Barbacki)[35]

produces a marked difference in carbide morphology. We cannot thus assume that interphase precipitation is necessarily associated with ferrite having a *K-S* relationship with the austenite in which it is growing, while fibrous carbides grow in a pearlitic fashion where the ferrite is unrelated to the parent austenite grain. This recent evidence points to the nature of the γ/α interface as the important factor influencing the observed carbide morphologies. It is augmented by such information as shown in Fig. 13 where, as the orientation of the boundary changes, the carbide morphology abruptly alters; the boundary in the interphase precipitate region exhibits small steps, which are absent in the fibrous region, where the interface is more irregular with local curvatures.

It is now recognized that the interface between two phases is a significant diffusion path, and that the diffusivity along a disordered boundary is greater than along a coherent or semicoherent low energy boundary. Thus circumstances could be expected where, as the temperature is lowered, the growth of low energy interfaces by step movement is replaced by incoherent interfaces with their increased capability for diffusion. This could explain the increased incidence of fibrous carbide growth in the molybdenum steel as the transformation temperature is lowered towards the nose at 750°C, and the reaction takes place more rapidly.

5. THE EFFECT OF ALLOYING ELEMENTS ON STRUCTURE

It will be already very apparent from the examples given that different alloying elements in steels greatly influence the type of carbide morphology encountered during direct transformation of austenite. In the main the alloying elements achieve this effect in two ways:

1) by altering the kinetics of the basic γ/α reaction

2) by changing the composition and structure of the carbide phase.

The addition of as little as 0.25 pct vanadium to an iron-0.1 pct carbon alloy causes the γ/α reaction to occur predominantly by stepped growth of ferrite with associated interphase precipitation of vanadium carbide. One important characteristic of these steels is that the reaction is extremely rapid, going to completion at the nose of the TTT curve in about 15 seconds,[29] and there is little change in speed as the vanadium content is increased up to 1 pct. The addition[36] of further alloying elements such as nickel, manganese or chromium has the effect of slowing down the transformation, and at the same time increasing the amount of fibrous vanadium carbide from as low as 2 pct up to 20 pct of the carbide phase for a 1.5 pct Mn addition, and up to 40 pct for 2 pct Cr. Steels containing titanium and columbium as the principal carbide forming elements exhibit similar behavior to vanadium steels *i.e.* rapid reaction and the formation of carbides isomorphous with vanadium carbide (fcc structure) mainly by interphase precipitation. In the case of steels containing titanium,[37] slowing down the reaction by use of further alloying elements increases the proportion of fibrous carbide.

In contrast, molybdenum steels[16] isothermally transform more slowly, and in any case require more alloying element to form Mo_2C (and M_6C) instead of cementite. The Mo_2C carbide forms commonly in fibrous form, although interphase precipitation of the same carbide occurs side by side with fibrous Mo_2C even in the same austenite grain. The Mo_2C interphase precipitate progresses in a needle or rod-like morphology which might be expected to change to a fibrous habit more readily than the plate shaped VC particles. It thus appears that when a steel transforms more slowly, fibrous carbide growth becomes more favored, and thus represents a closer approach to equilibrium in contrast to repeated nucleation of particles at the γ/α interface which is energetically more demanding.

However, this cannot be a full explanation, as a tungsten steel[21] of similar atomic concentration to the molybdenum steel (Fe-2 at. pct Mo-1 at. pct C) has similar reaction kinetics, but exhibits only a small amount of fibrous tungsten carbide on transformation. Instead over the transformation range 650–850°C the interphase reaction predominated, but usually with the precipitation of $(FeW)_6C$ a complex cubic carbide *not* W_2C (which is isomorphous with the hexagonal Mo_2C). In molybdenum steels M_6C can form at the higher transformation temperatures, but the normal precipitate observed is Mo_2C. Likewise in high chromium steels the reaction is slow, *e.g.* 100 minutes to full transformation at 700°C in a 12 pct Cr alloy, but the product is a complex mixture of ferrite with fibrous $M_{23}C_6$ (a cubic carbide) and also interphase precipitation of the same carbide. One is thus forced to conclude that there must be crystallographic factors influencing growth of the carbide in addition to the kinetic factor. It is particularly relevant to compare vanadium carbide (fcc VC) with molybdenum carbide (hexagonal Mo_2C). The orientation relationships of these two carbides with both γ and α-iron are known, and using accepted lattice parameters, the lattice mismatch factors can be calculated as shown in Table I, based on data by Davenport *et al*,[18] Harding[38] and Dyson *et al*.[39]

These results indicate more favorable crystallographic conditions for VC to grow in ferrite than in austenite, whereas in the case of Mo_2C the conditions are similar in both ferrite and austenite. Consequently VC would be expected to favor interphase growth where it is essentially growing in ferrite with the observed ferrite orientation relationship. As has already been pointed out, this carbide normally adopts only one of the variants of the orientation relationship, forming as platelets on that cube plane of ferrite most nearly parallel to the γ/α interface, possibly to maximize the effectiveness of the γ/α boundary diffusion

Table I. Lattice Mismatch for Vanadium and Molybdenum Carbides in Ferrite and Austenite

	VC		Mo_2C	
Matrix	Orientation Relationship	Misfit, Pct	Orientation Relationship	Misfit, Pct
α	$[100]_c//[1\bar{1}0]_\alpha$	2.6	$(00\,1)_c//(011)_\alpha$	16.5
	$[010]_c//[110]_\alpha$	2.6	$(01.0)_c//(01\bar{1})_\alpha$	28.3
	$(001)_c//(001)_\alpha$	45.2	$(2\bar{1}.0)_c//(100)_\alpha$	4 7
γ	cube/cube	16.0 all directions	$(00.1)_c//(111)_\gamma$	14.1
			$(11.0)_c//(1\bar{1}0)_\gamma$	18.4
			$(1\bar{1}.0)_c//(11\bar{2})_\gamma$	−11.2

path or as a result of surface energy considerations. The greater preponderance of Mo_2C fibers in the molybdenum steel is probably due in part to the nature of the misfit between Mo_2C and ferrite where there is a low degree of misfit in only one direction, in contrast to VC where there are two directions of relatively low misfit and as a result the habit is normally plate-like.

In vanadium steels, it has been observed[40] that in localized regions vanadium carbide platelets are replaced by short fibers (Fig. 17) which remain parallel to the original plates of VC, and appear to arise simply from prolonged growth of these particles. This might happen if fluctuations occurred such that localized regions of the γ/α boundary moved not by a step mechanism but by slow break away in a direction *normal* to the interface; the fibrous growth would be expected to cease when the step mechanism of interface growth was resumed. It is probable that such events are more likely during continuous cooling than during isothermal transformation, because the reaction takes longer to go to completion in the former case, allowing more opportunity for growth fluctuations to occur.

There is a small group of alloying elements, notably silicon, aluminum and cobalt, which accelerate the kinetics of the γ/α reaction, at least at the higher transformation temperatures.[8] Silicon and aluminum appear to increase both the rates of nucleation and growth of ferrite, while cobalt increases only the rate of nucleation. Recent work[41] has shown that these effects on the γ/α reaction are also reflected in an increase in strength of the ferrite, assumed to be partly from increased dispersion hardening and partly from additional solution hardening.

6. STABILITY OF CARBIDE DISPERSIONS IN FERRITE

6.1 Coarsening Kinetics

The initial state of the dispersion of vanadium or titanium carbide produced during the γ/α transformation is so fine, and the reaction is so rapid, that it is of considerable interest to know the effects of further aging at the transformation temperature. Batte[36] working with an Fe-1 pct V-0.2 pct C alloy found that the original banded structure had disappeared after one hour at 725°C, while Freeman[37] showed that an Fe-0.5Ti-0.1 pct C alloy maintained the banded structure up to 40 hours at 700°C, although a further 30 minutes at 800°C caused the banding to disappear entirely. At lower temperatures, for example 600°C, the banded structure still persists in Fe-V-C after 500 hours.[42]

The Lifshitz-Wagner theory of diffusion-controlled particle coarsening is often applied to solid state structures, although it is strictly concerned with spherical particles in fluid matrices. The relationship is of the form

$$(r_t^3 - r_0^3) = \frac{K}{RT} V^2 CD\gamma t \qquad [1]$$

where r_0 and r_t are the mean particle radii at zero time and time t; D is the diffusivity of the solute in the matrix; γ is the particle/matrix interfacial energy; C is the concentration of solute in equilibrium with

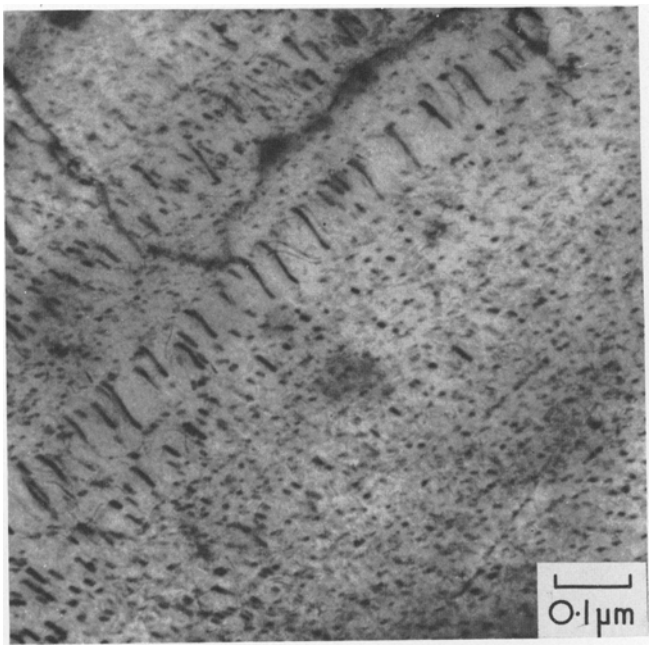

Fig. 17—Transition from interphase to fibrous vanadium carbide growth in an isothermally transformed vanadium steel. Thin foil EM. (Batte)[29]

a particle of infinite size; V is the molar volume of the precipitate, and K is a constant. The coarsening of Mo_2C particles in tempered ferrite[43] follows $t^{1/3}$ kinetics in qualitative agreement with Eq. [1], and has an apparent activation energy near that for Mo diffusion in ferrite. However studies of banded VC coarsening in ferrite using the field ion microscope showed that $t^{1/2}$ kinetics were followed,[44] indicating an interface reaction controlled coarsening in accordance with the equation,

$$(r_t^2 - r_0^2) = \frac{64\, CS\gamma V t}{81\, kT} \qquad [2]$$

where S is the average solute concentration in the matrix at a long distance from the nearest particle.

More recent work by Dunlop and Honeycombe[45] on Fe-V-C and Fe-Ti-C alloys coarsened after transformation at 725°C has shown that $t^{1/5}$ kinetics describe the process accurately. This time dependence was predicted by Kraye[46] and later by Ardell[47] for the coarsening of particles lying on dislocations, when the following equation applies:

$$(r_t^5 - r_0^5) = \frac{K'}{RT} V^2 CD_d q\gamma N t \qquad [3]$$

where D_d is the diffusion coefficient for dislocation pipe diffusion; q is the effective cross-sectional area of the dislocation pipe diffusion path; N is the number of dislocations intersecting each particle (assumed to be constant); K' is a constant. High resolution electron microscopy confirms that the particles which preferentially coarsen lie on dislocations and that as a result an irregular network of particles gradually replaces the fine bands of precipitate formed during the phase transformation (Fig. 18(*a*)). The dislocations in the structure most probably occur as a result of the volume change during the phase transformation, and were not initially sites for carbide nucleation; instead particles formed by the interphase

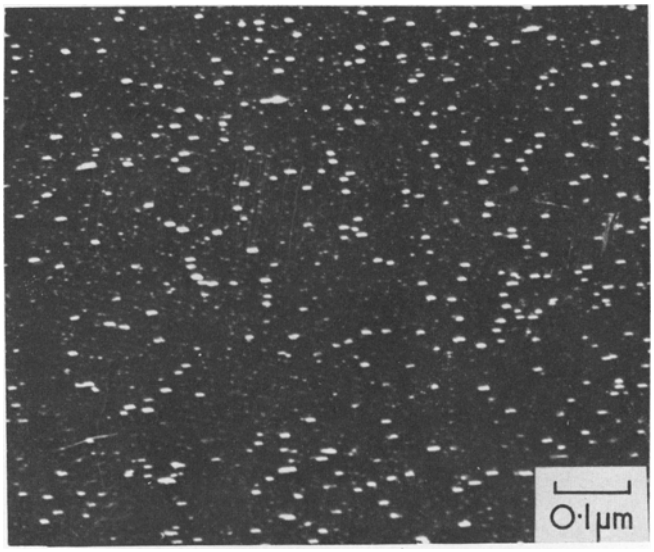

(a)

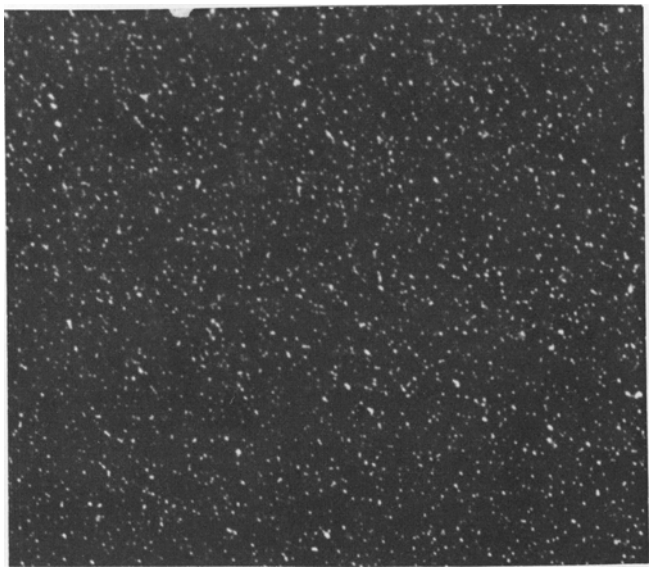

(b)

Fig. 18—Precipitate dark field electron micrographs of (*a*) Fe-0.4V-0.08C (*b*) Fe-0.18V-0.13Ti-0.08C isothermally transformed and held 15 min at 725°C. (Dunlop)[18]

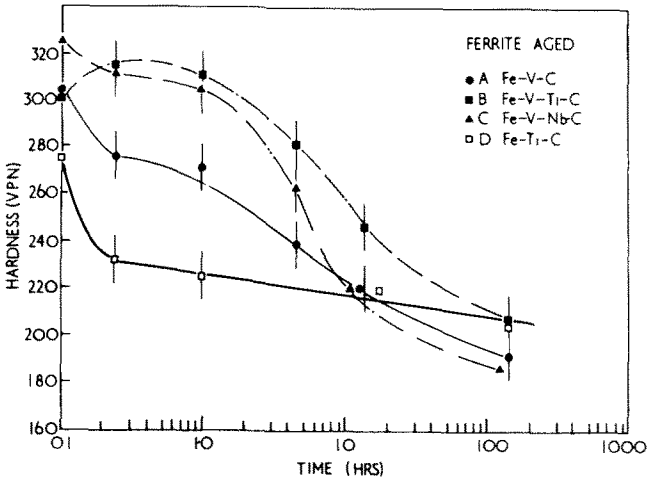

Fig. 19—Softening of simple ternary and quaternary alloys after aging at 725°C. (Dunlop)[48]

mechanism, which seem to be coherent with the matrix in the early stages of growth, possess strain fields which interact with those of dislocations. This results in particle pinning by the dislocations, followed by selective growth of some particles enhanced by pipe diffusion of solute along the dislocations.

6.2 The Effect of Carbide Composition on Coarsening

The fcc carbides VC, TiC, CbC are all precipitated in the appropriate alloys during the γ/α transformation, moreover they are mutually soluble in each other, so the possibility of obtaining solid solution carbide phases exists. Experiments have been carried out by Dunlop[48] on the coarsening of a series of alloys as follows:

Table II. Iron-Base Alloys for Carbide Coarsening Studies

	Composition			
Alloy	C	V	Ti	Cb
A				
wt pct	0.08	0.40	–	–
at. pct	0.37	0.44	–	–
B				
wt pct	0.08	0.18	0.13	–
at. pct	0.37	0.20	0.15	–
C				
wt pct	0 07	0 15	–	0 26
at pct	0 33	0 17	–	0 16
D				
wt pct	0 09	–	0 33	–
at pct	0 42	–	0 38	–

All four alloys were solution treated 24 hours at 1300°C followed by water quenching; they were then further solution treated 15 minutes at 1300°C after which they were transformed at 725°C for 5 minutes, then subsequently aged for increasing times at 725°C. Fig. 19 plots the changes in hardness of the four alloys up to 150 hours. It is clear that the simple ternary alloys *A* and *D* initially soften more rapidly than the alloys *B* and *C* which each contain two carbide forming elements, however after 150 hours all four alloys had reached a similar hardness around 200 VPN. The largest differences occurred early in the aging process, and even after 15 minutes electron microscopy revealed marked differences in carbide dispersion between alloys *A* and *B* and also between alloys *B* and *D*. Fig. 18(*a*) and (*b*) are precipitate dark field electron micrographs of alloys *A* and *B* after 15 minutes at 725°C, the more rapid coarsening of alloy *A* is evident, the coarse particles of VC lying on an irregular dislocation network. The simple titanium steel coarsened even more rapidly. To put the matter on a more quantitative basis, particle size distributions of carbides in the alloys were determined from micrographs such as those in Fig. 18. Typical results are shown in Fig. 20 for alloys *A*, *B* and *D* after 15 minutes at 725°C, the mean particle sizes being 2.9, 2.1 and 6.6 nm respectively. After 15 hours the distributions were again determined as shown in Fig. 21 when the

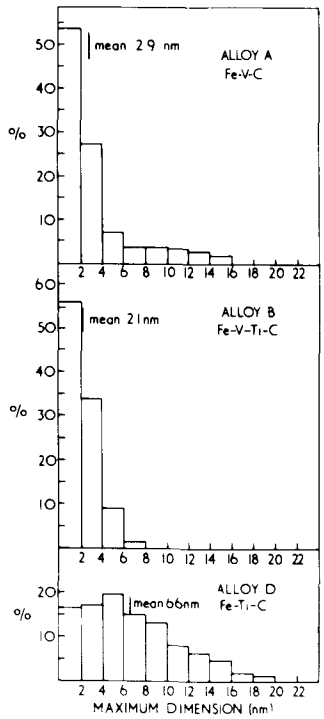

Fig. 20—Particle size distribution after aging alloys *A*, *B* and *D* for 15 min at 725°C. (Dunlop)[18]

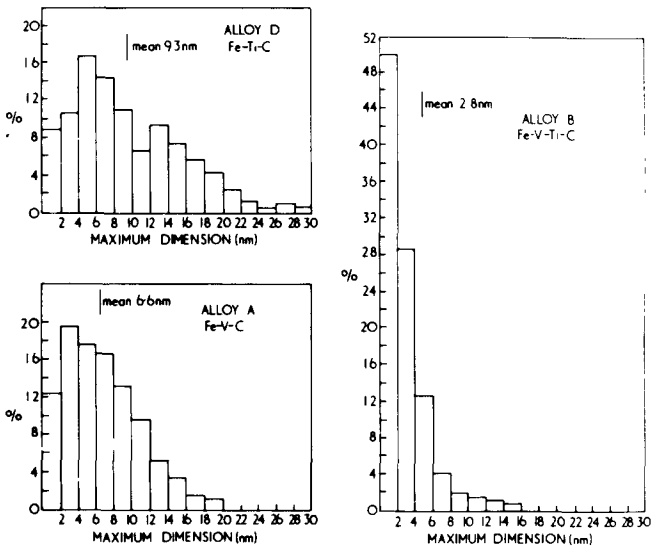

Fig. 21—Particle size distribution after aging alloys *A*, *B* and *D* for 15 h at 725°C. (Dunlop)[18]

mean particle sizes had risen to 6.6, 2.8 and 9.3 nm respectively. The much slower growth rate of the mixed carbide alloy is thus very evident.

It should be emphasized that in all these alloys the initially formed precipitate was banded, although careful tilting of thin foil specimens is necessary to establish this fact. However measurements on both the band spacing and the particle size at the same time were only possible after transformation at 800°C. The average dispersion parameters for alloys *A*, *B* and *D* are given in the table.

It should be noted that the band spacing in *A* was coarser than in *B* or *D*, whereas on aging the alloy *D* coarsened to the greatest degree (Figs. 20, 21). This implies that different factors determine the band spacing

Table III. Dispersion Parameters in Ternary and Quaternary Alloys (800°C)

Alloy	Mean Sheet Spacing, nm	Mean Particle Size, nm
A (Fe-V-C)	50-60	7-10
B (Fe-V-Ti-C)	17-27	4-5
D (Fe-Ti-C)	20-25	6 5-10.5

to those controlling the subsequent coarsening of the dispersion. There is some evidence that titanium diffuses more readily in ferrite than does vanadium,[49] which could thus explain the observed differences in coarsening kinetics. On the other hand, the initial spacing of the dispersion could well be determined by the thermodynamic driving force for the $\gamma \rightarrow \alpha$ reaction. As the free energy of formation of TiC is significantly more negative than that of VC, the transformation in the titanium steel would be expected to have the higher driving force. Unfortunately these ferritic reactions in vanadium and titanium steels occur very rapidly, with the result that there are as yet no accurate comparative kinetic data to be able to check this assumption.

The implication in the above experiments that the two carbides form one solid solution is an assumption which needs verification, although for similar carbides in the massive state there is reliable X-ray evidence for such solid solubility. Direct evidence has now been provided by the use of field ion microscopy which not only allows resolution of the finest carbide particles in an iron matrix, but also is capable of atomic resolution. Moreover by the use of an atom probe in conjunction with a field ion microscope, it is possible to field evaporate individual atoms from carefully selected atomic regions, and obtain positive identification by use of a time-of-flight mass spectrometer. Dunlop and Turner[50] have applied this method to the alloy *B* above, containing both vanadium and titanium. Transformation at 725°C for 5 minutes produced carbide particles with an average particle size of around 2 nm, which were shown by use of the atom probe to contain both V and Ti. Precise analysis at this size level is still difficult and usually matrix ions are included, however if the particle size is substantially increased to about 40 nm (Fig. 22(*a*)), a complete atom-by-atom analysis of the particles is possible as shown in Fig. 22(*b*). Such a particle readily provides between 250 and 400 atoms for analysis so that good statistical determination of individual particle composition is possible. It should be noted from Fig. 22(*b*) that the particles did not contain any iron atoms. The metal/carbon atomic ratios are consistent with those obtained by other workers in bulk compounds, $VC_{0.84}$, $TiC_{0.84}$ and $(VTi)C_{0.84}$. The fine particles precipitated in the steel used in this investigation were shown to approximate to the formula $(V_{0.45}Ti_{0.55})C_{0.84}$, conclusive evidence for the formation of solid solution carbides in steels containing more than one carbide forming element.

7. THE EFFECTS OF DEFORMATION ON THE γ/α TRANSFORMATION

It is important to examine the effects of plastic deformation on the subsequent transformation of austenite, as many modern steels are hot rolled in the

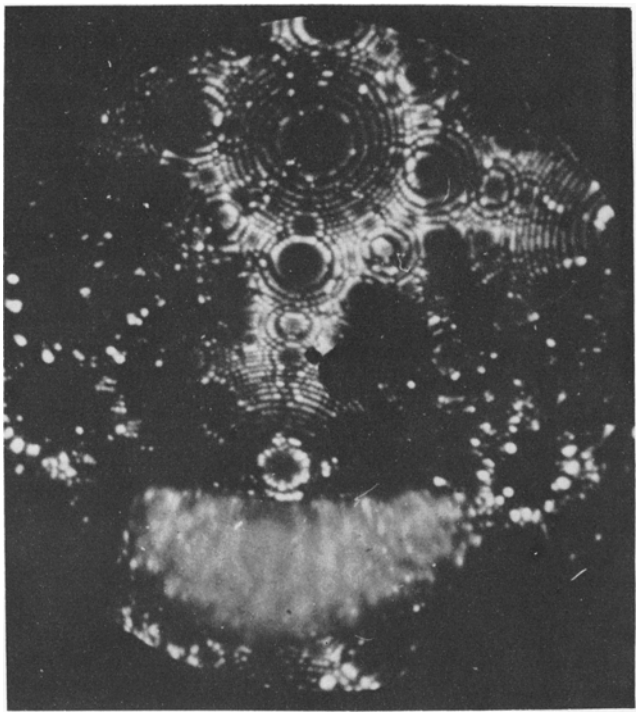

(a)

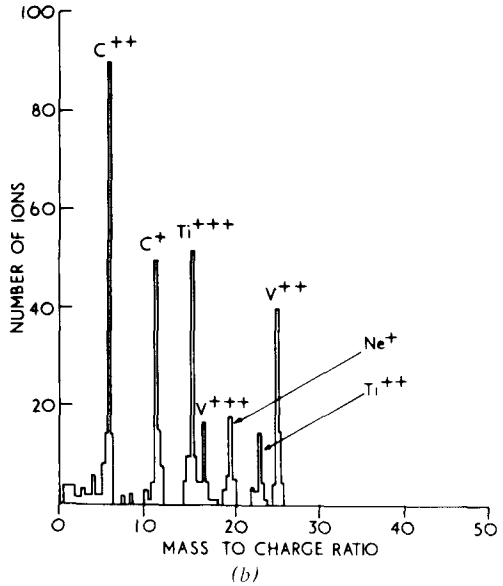

(b)

Fig. 22—(*a*) Field-ion micrograph of alloy *B* transformed and aged 27 h at 800°C. Image diameter 100 nm, particle size 40 nm. (*b*) Spectrum of ions detected in atom probe from a particle similar to that in (*a*). (Dunlop and Turner)[50]

austenitic condition down to quite low temperatures, and even into the transformation range. Controlled rolling is now an accepted method of achieving better and more consistent properties in wrought steels. Many experiments have been done on the controlled rolling of micro-alloyed steels mainly with a view to optimizing procedures, however there has been much less work providing basic information on the effects of deformation on the phase transformation.

Work with stable austenitic steels has shown that plastic deformation at room temperature accelerated the precipitation reactions which occur on aging[51,52] a trend which is observed in many alloy systems. Turning to transformable austenite, Smith and Siebert[53] have found that deformation of the austenite increases the limiting cooling rate necessary to avoid transformation to ferrite, while both the bainite and martensite start temperatures were raised. Recent Russian[54,55] work has shown that the high temperature decomposition of austenite in a range of alloy steels was accelerated by plastic deformation, but at lower transformation temperatures in the ferrite range the reaction could either be accelerated or retarded depending on the temperature at which the deformation was carried out.

Walker,[56] using AISI 4337 (1.4Ni-1Cr-$\frac{1}{4}$Mo-0.35 pct C) and a simple 5 pct Cr-0.2 pct C steel, has demonstrated that plastic deformation in tension of the metastable austenite in the bay at 550°C has a large effect on the transformation at the nose of the TTT curve (650°C). Fig. 23(*a*) illustrates the accelerating effect of deformation on the phase transformation in AISI 4337; while the undeformed steel begins to transform in 900 seconds at 650°C, 30 pct tensile deformation at 550°C causes the steel to commence transforming in less than 100 seconds. In the undeformed steel the ferrite reaction commences almost exclusively at the grain boundaries, however 30 pct deformation at 550°C causes intragranular nucleation which refines the ferrite grain size. The pearlite reaction occurred in both the deformed and undeformed steel, but the colony size was reduced by about one half (~5 microns) in the deformed specimen. In addition a substructure appeared in the colonies involving the formation of ferrite sub grains with slight discontinuities in the cementite lamellae at the sub-boundaries.

That plastic deformation of the austenite caused nucleation of carbides prior to transformation, was demonstrated by raising the deformation temperature above the nose to 750°C. After transformation the product was still a ferrite-pearlite aggregate, but the ferrite contained a fine carbide dispersion arranged on an irregular network (Fig. 24). Electron diffraction measurements showed that the carbide was $M_{23}C_6$ which forms readily in austenite, but would not be expected to form during transformation of AISI 4337 from austenite to ferrite and carbide. The conclusion is that the networks of $M_{23}C_6$ nucleate on dislocation sub-boundaries during the hot deformation of austenite, when sub-grains are formed as a result of dynamic recovery.

The effect of deformation of the austenite prior to transformation is perhaps best illustrated by work on an iron-1 pct vanadium-0.2 pct C alloy similar to

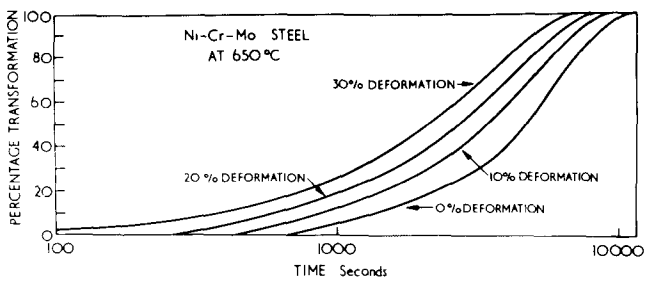

Fig. 23—Effect of plastic deformation at 550°C on the rate of transformation of austenite in AISI 4337 at 650°C. (Walker)[56]

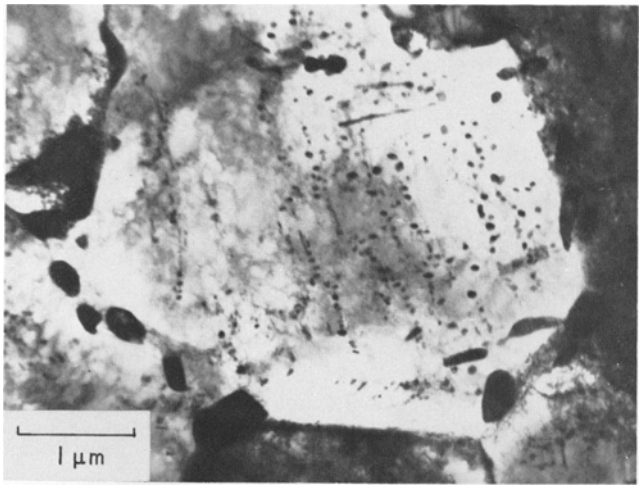

Fig. 24—AISI 2337 deformed 25 pct at 750°C prior to transformation at 650°C. Irregular $M_{23}C_6$ carbide network in the ferrite phase. Thin foil EM. (Walker)[56]

that used to study banded precipitation of vanadium carbide, where because of the rapidity of the transformation, the alloy must be deformed at a higher temperature, *e.g.* 875°C prior to transformation at 700°C. As little deformation as 8 pct in tension reduced the ferrite grain size from about 70 microns down to 15 microns; it is assumed that this resulted from nucleation of ferrite both at the austenite grain boundaries and within the grains. Fig. 25 (*a*)–(*c*) illustrates the changes in ferrite grain size as a result of holding at 875°C then deforming prior to transformation. Electron microscopy showed that vanadium carbide precipitated first in the austenite at 875°C, as might be expected after a solution treatment at a much higher temperature (1150°C), regardless of whether the austenite was deformed. This precipitation of VC was much coarser than that formed furing the γ/α transformation as illustrated in Fig. 26, where the difference in size is 70–100 nm for precipitation in austenite compared with about 10 nm for precipitate formed during transformation at 700°C. As in the case of AISI 4337, it is assumed that nucleation has taken place on dislocation networks, which have disappeared subsequently during the γ/α transformation. There is also extensive precipitation of vanadium carbide on prior austenite grain boundaries.

Turning to the vanadium carbide formed during the γ/α transformation, deformation decreased the proportion of interphase precipitation and increased the incidence of fibrous vanadium carbide, which is unexpected in so far as fibers are usually favored by a slowing down of the γ/α reaction. One assumption is that the increase in dislocation density of the austenite modifies the interphase boundary making it of higher energy, at least in some regions, where fibrous vanadium carbide then grows preferentially.

8. MECHANICAL PROPERTIES OF DIRECTLY TRANSFORMED STEELS

The structural work described earlier in this paper shows that in selected groups of alloy steels it is possible to obtain by direct transformation of austenite,

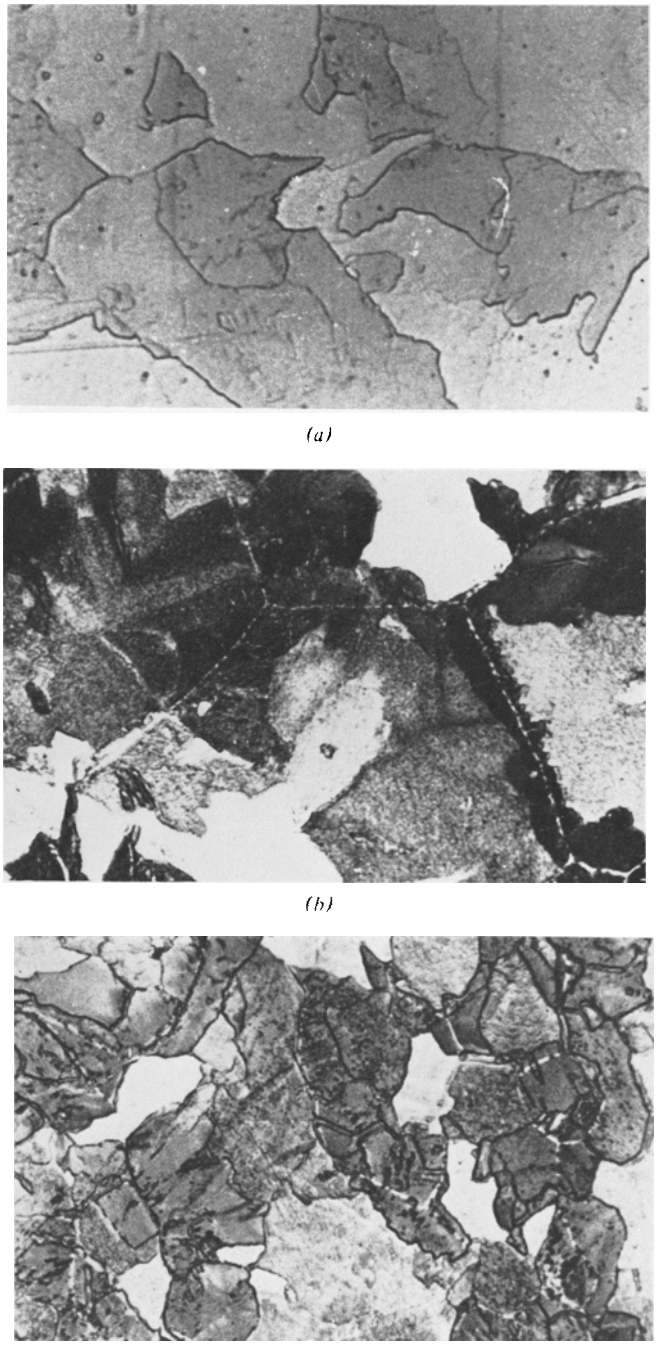

(*a*)

(*b*)

(*c*)

Fig. 25—Effect of deformation and/or aging on the transformation of Fe-1V-0.2C at 700°C. (*a*) Directly transformed at 700°C, (*b*) aged at 875°C prior to transformation, (*c*) deformed 8 pct at 875°C prior to transformation. Optical micrographs, magnification 900 times. (Walker)[56]

ferritic matrices containing very fine carbide dispersions. These dispersions are similar (but by no means identical) to those obtained in many quenched and tempered alloy steels, so it is obviously important to determine the mechanical properties. We shall first briefly discuss the main strengthening mechanisms, and then show the range of properties possible as the volume fraction and state of the carbide dispersion is varied by choice of composition and heat treatment.

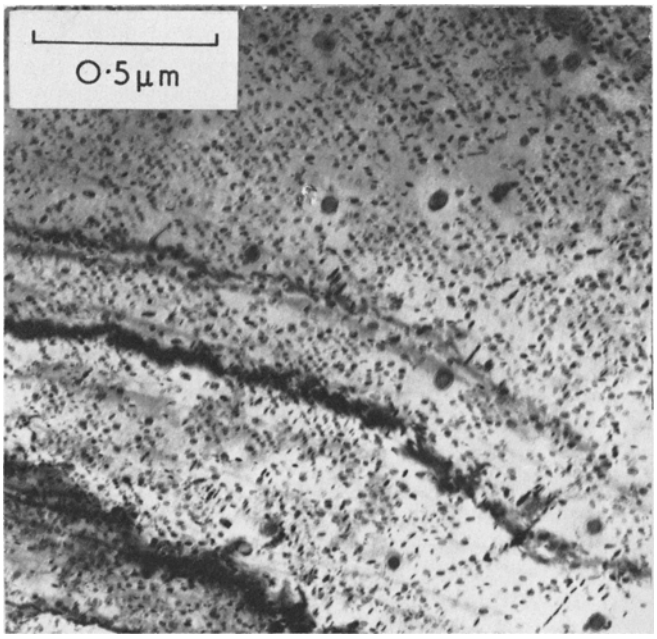

Fig. 26—Same treatment as Fig. 25(*b*), showing the two vanadium carbide dispersions. Thin foil EM. (Walker)[56]

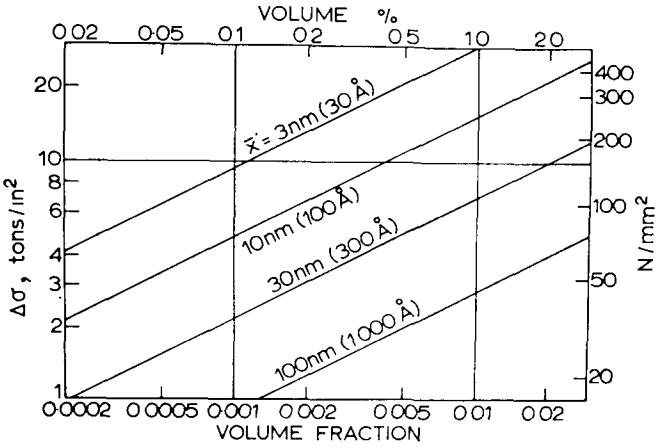

Fig. 27—Application of the Orowan-Ashby relationship to a ferrite matrix. (Gladman et al)[61]

8.1 Strengthening Mechanisms

There are a number of important metallurgical variables which will determine the strength levels achieved in directly transformed ferritic steels, but these are effective because of changes in one or more of the three basic strengthening mechanisms, which all contribute to the observed mechanical properties

1) grain size
2) solid solution hardening
3) dispersion strengthening.

If the bainite transformation is included, the dislocation density must also be listed as a source of strengthening.

In low carbon steels the grain size strengthening is a predominant factor as defined by the Hall-Petch relationship

$$\sigma_y = \sigma_0 + k_y d^{-1/2} \qquad [4]$$

where σ_y is the yield stress and d the grain diameter.

However achievement of fine grain sizes requires the combined use of controlled hot rolling and fine carbide dispersions which pin the boundaries and inhibit recrystallization and grain growth. Solid solution hardening for a given steel is essentially determined by the chemical composition, and is relatively uninfluenced by heat treatment. The third mechanism, dispersion strengthening, is the most relevant to the present paper.

Gladman *et al*[57] have applied the Orowan-Ashby model of dispersion hardening to high strength low alloy steels with dispersions of columbium and vanadium carbides using the relationship

$$\tau = \frac{1.2\,G\mathbf{b}}{2.36\,\pi L} \ln \frac{\overline{X}}{2\mathbf{b}} \qquad [5]$$

where τ is the resolved shear stress for plastic flow, G is the shear modulus of the matrix, $\mathbf{b}$ = Burgers vector, L is the inter-particle spacing, and $\overline{X}$ is the mean planar intercept diameter of the precipitate. Taking values for G = 5200 tsi (80,309 MNm^{-2}) and $\mathbf{b}$ = 0.28 nm, the yield stress increments ($\Delta\sigma$) can be calculated for different average particle sizes as the volume fraction of precipitate is changed (Fig. 27); these are results predicted for an iron-base matrix. The authors found that steels containing 0.03–0.04 wt pct Cb showed increments in yield stress of around 90 MNm^{-2} (~6 tsi) which was found to be in reasonable agreement with the theory. Variation of columbium contents up to 0.04 pct also gave results which fitted the theory. The strengthening of the fine precipitates thus gave a modest but useful contribution to the overall yield stress. It should however be pointed out that much higher volume fractions of carbide can be obtained with vanadium and titanium carbides which are more soluble in austenite than columbium carbide. These alloys are considered in the next section.

8.2 Basic Work on Vanadium and Titanium Steels

An interesting comparison has been made of the mechanical properties of the phases occurring in a simple vanadium steel (0.85 pct V-0.23 pct C) when isothermally transformed between 600 and 850°C; at 650°C and below, upper bainite coexists with ferrite containing a VC dispersion. Fig. 28 gives the relative micro-hardness of bainite and ferrite found at 650°C showing that the ferritic phase is much stronger. It is clear that the mechanical properties of ferrite produced between 650 and 850°C are likely to be of considerable interest.

The strength of such materials is best evaluated by assuming that the major contributions to the strength, *viz*. grain size, solid solution strengthening and dispersion strengthening are additive, thus following Pickering and Gladman's[58] approach to ferrite/pearlite steels, the yield stress σ_y is defined by the following equation

$$\sigma_y = \sigma_0 + \sum k_i r_i + \sum k'_j c'_j + k_y d^{-1/2} \qquad [6]$$

where σ_0 is the inherent friction stress of the matrix, the second term represents the solid solution strengthening of several components while the third term arises from dispersed phases, and the final term is the familiar grain size term from the Hall-Petch

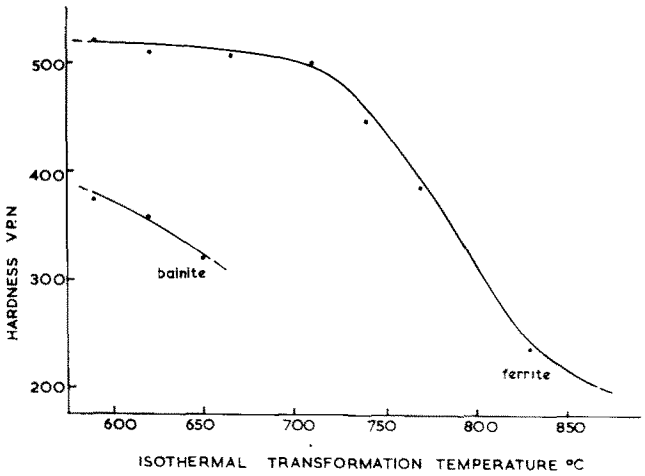

Fig. 28—Microhardness of phases formed by isothermal transformation of a 0.85 pct V 0.25 pct C steel. (Batte and Honeycombe)[29]

equation. The approximate value of σ_0 can be taken from work on pure iron, from which a value as low as 20 MNm^{-2} could be reasonably used. The individual element contributions to solid solution hardening have been determined by regression analysis of a large number of commercial steels. The grain size strengthening is well documented, and the constant k_y is known, consequently the contribution of dispersion strengthening to the overall yield stress can be obtained by subtraction of the other three contributions, which eliminates the need for difficult and often inaccurate determination of particle sizes and distributions to enable the Orowan-Ashby relationship to be used. Such an analysis has been applied to a series of simple vanadium steels,[29] where, by changing the (vanadium + carbon) concentrations, the volume fraction of vanadium carbide precipitate was varied from 0.23 to 1.23 pct. The steels were all given similar heat treatments, *viz.* austenitized at 1200°C then quenched into tin baths held at transformation temperatures between 725 and 825°C for sufficient time to complete transformation. Tensile tests were carried out at room temperature, and the results analyzed to determine the various contributions to the yield stress. Table IV gives some of the data obtained from which it can be seen that

a) dispersion strengthening of the higher vanadium carbon alloys can provide a major part of the strength, up to 600 MNm^{-2};

b) the dispersion strengthening reduces rapidly as the transformation temperature is raised;

c) the dispersion strengthening increases with the volume fraction of carbide precipitate.

This data on the mechanical properties of vanadium steels should be related to the quantitative metallographic data on the vanadium carbide dispersions observed in these steels and summarized in Fig. 8(*a*) and (*b*). It should be emphasized that these experiments were designed to determine the effect of the dispersion of vanadium carbide on the strength of the steels, and no attempt was made to optimize the grain size and solid solution components, which did not vary much in these experiments.

8.3 Metallurgical Variables Influencing Mechanical Properties

We have now reached a point where it is possible to summarize the variables which determine the mechanical properties obtainable in alloy steels by direct transformation of austenite, and to indicate the factors which should be taken into account in designing steels to exploit the observed phenomena.

8.3.1 The Choice of Composition. While this is a complex matter, we can progress by limiting consideration to two aims:

a) the achievement of a relatively high volume fraction of a fine carbide dispersion,

b) the attainment of γ/α reaction kinetics which accelerate ferrite formation and thus minimize the oc-

Table IV. The Mechanical Properties of Isothermally Transformed Vanadium Steels

			MN m^{-2}			
Alloy	Vol. Fract., Pct	Trans. Temp., °C	Yield Stress, σ_y	Fric. Stress + Solid Solution, $\sigma_0 + \sigma_{ss}$	Grain Size Strength, $k_y d^{-1/2}$	Dispersion Strength, $\sigma_{disp.}$
*C*1	1.23	725	843	19.6	236	587
1.04 wt pct V		750	843	19 6	215	608
0 20 wt pct C		775	667	19 6	194	453
		800	549	19.6	168	362
		825	441	24 5	136	280
*C*2	0.93	725	755	19.6	177	559
0.75 wt pct V		750	637	19 6	161	457
0.15 wt pct C		775	539	19 6	154	366
		800	451	24.5	126	301
		825	353	29.4	102	222
*C*3	0.55	725	647	19 6	236	391
0 48 wt pct V		750	559	19 6	215	324
0.09 wt pct C		775	441	19 6	228	228
		800	363	2 5	168	171
		825	284	3.0	136	119
*C*5	0.23	750	392	19 6	215	157
0.55 wt pct V		775	333	19 6	194	120
0 04 wt pct C						

currence of bainite or martensite on cooling.

To obtain a suitable dispersion strengthened ferrite it is necessary to have alloy carbides (or nitrides) which are soluble in austenite. Fig. 29 shows the solubility products (in at. pct) in austenite of several of the most familiar carbides and nitrides which occur in alloy steels. In all cases the carbides have greater solubilities in austenite than the corresponding nitrides, and the most useful carbides would appear to be those of Cr and Mo. However the concentrations of Cr and Mo needed to form dispersion of alloy carbides slow down the γ/α transformation to a degree that the dispersions are often fairly coarse and not easily controlled. In contrast, V, Ti and Cb form alloy carbides at much lower concentrations of alloying element which do not drastically alter the reaction kinetics. Moreover the latter elements tend to encourage the finer banded carbide dispersions, whereas Cr and Mo promote the growth of coarser fibrous and pearlitic carbides. However these considerations do not exclude the combined use of elements, *e.g.* chromium in association with vanadium or titanium; the latter being stronger carbide formers can result in VC or TiC precipitation in the presence of high chromium concentrations. Typically a $\frac{1}{2}$Cr-$\frac{1}{2}$Mo-$\frac{1}{4}$V-0.1C steel on isothermal transformation in the range 650–770°C gives a very fine dispersion of VC, while a 4 pct Cr-1 pct V-0.2 pct C steel also has a VC dispersion after a similar treatment.

The rapid reaction kinetics required for the ferrite reaction are achieved by the presence of V, Ti, Al and Si, and steels based on these elements can fully transform at the nose of the TTT curve in less than half a minute. However the addition of Mn, Ni or Cr will slow down the reaction and make the formation of other structures more likely, particularly during continuous cooling. It is thus clear that in directly transformed ferritic steels one should be aiming for the *reverse* of hardenability. Those elements needed in quenched and tempered steels such as nickel and manganese to achieve martensitic structures in thick sections are disadvantageous in ferritic steels in so far as they slow down the ferrite reaction to a point where the dispersion strengthening is much lower than can otherwise be achieved. Moreover they make it more likely that bainite or martensite will form instead of ferrite during rapid cooling. However, as they depress the temperature at which the ferrite reaction starts, in small concentrations they can decrease the dispersion parameters in continuously cooled steels, and thus be advantageous.

8.3.2 The Austenitizing Temperature. To fully develop a carbide dispersion it is first necessary to take into solution in austenite the appropriate carbide phase, and as implied in Fig. 29, this requires temperatures between 1150 and 1300°C for VC, TiC and CbC. Chromium and molybdenum carbides can be dissolved at rather lower temperatures. While the use of these high temperatures is necessary, it can lead to excessive austenite grain growth which can be inhibited by not allowing all carbide particles to be taken into solution; if these residual particles are below a critical size r_{crit}, the grain boundaries remain pinned according to the relationship determined by Gladman[59]

$$r_{crit} = \frac{6\overline{R}_0 f}{\pi}\left(\frac{3}{2} - \frac{2}{Z}\right) \qquad [7]$$

where f is the volume fraction of particles, $\overline{R}_0$ is the matrix grain radius, and Z is the ratio of the radii of the growing grain to the matrix grain. The driving force for grain growth exceeds the boundary pinning force when r exceeds r_{crit}; so fine particles are needed to restrain grain growth, but as they coarsen they become less effective in this role. In controlled micro-alloyed steels, the effects of grain growth at high temperatures are rapidly removed by the hot working process, but in the absence of deformation, careful attention must be given to control of grain growth at the solution temperature.

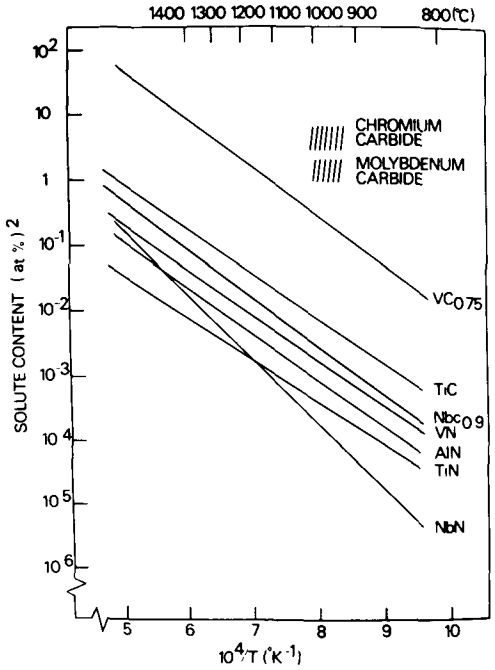

Fig. 29—Solubility products of carbides and nitrides in austenite. (Aronsson)[64]

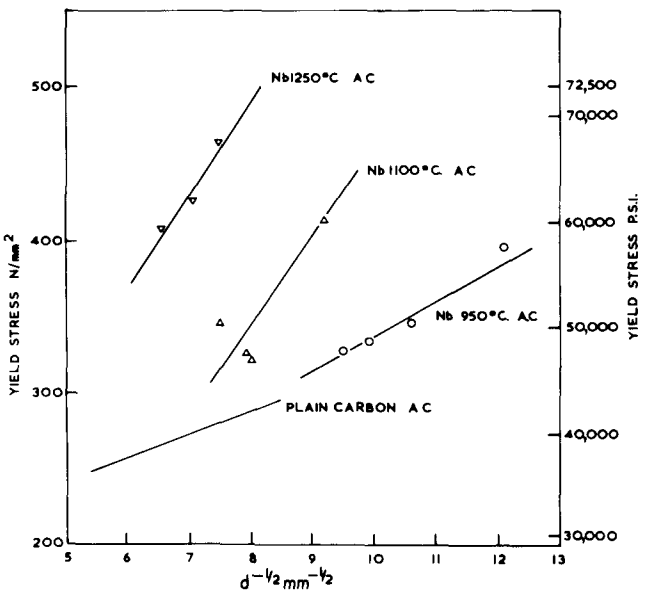

Fig. 30—The effect of 0.09 pct Cb on the strength of an 0.1 pct C-0.6 pct Mn steel. (Gladman et al)[61]

8.3.3 Rate of Cooling. It is highly desirable to cool rapidly from the solution temperature to avoid premature precipitation of carbides in austenite. Rapid cooling to room temperature is a practical alternative to quenching into baths for isothermal transformation, but it would be necessary to control the rate of cooling carefully to avoid formation of bainite or martensite. This achieved, then the ferrite formed at the highest cooling rates has the highest strength, in part because of the finer grain size achieved, but also because the carbide dispersion formed during transformation is also finer.[60]

8.3.4 Transformation Temperature. If isothermal transformation is the chosen heat treatment, then clearly the lower the temperature the higher will be the strength level achieved, but as in normal tempering, a treatment temperature should be chosen that gives the required balance between strength and ductility. The ferrite reaction in most suitable compositions occurs rapidly, but further control of properties is achieved by overaging at the transformation temperature.

9. MICRO-ALLOYED STEELS

Perhaps the best practical example of the application of direct transformation of austenite to obtain steels with useful properties is the important group of micro-alloyed steels, which owe their effectiveness to close control of composition, and the use of controlled rolling techniques to achieve fine grain size in the austenite prior to transformation and in the ferrite subsequently.[61,62] The micro-alloying additions are normally columbium, vanadium and titanium, either individually or in combination, the concentration rarely exceeding 0.1 wt pct. The role of these additions is primarily a result of their tendency to form both in austenite and ferrite, fine dispersions of alloy carbides which influence the working and heat treatment procedure in a complex way. The main factors are as follows:

1) At high austenitizing temperatures, residual alloy carbide particles are located at the grain boundaries, and limit the process of grain growth.

2) During hot rolling the particles influence the rate at which dynamic recrystallization can occur.

3) As the temperature falls during rolling, alloy carbide precipitation occurs primarily on dislocation networks and boundaries, and plays an increasingly controlling role in the recrystallization of the austenite during working, determining in conjunction with the rolling schedules the final austenite grain size and shape prior to transformation.

4) When the γ/α transformation occurs, further alloy carbide precipitation takes place in the form of interphase precipitation.

5) If the final deformation temperature is very low, the ferrite is formed during deformation and some alloy carbide particles will nucleate on dislocations formed in the ferrite.

Consequently in the finished steel the alloying elements influence the mechanical properties in two main ways; firstly they help in achieving very fine grain sizes, and secondly there is a substantial contribution to strength by the fine carbide dispersion. The precipitation of carbides in the austenite is primarily of use in controlling the grain size of the austenite, and, by inheritance, that of the ferrite. In the finished steel this dispersion is recognized as a network which probably does not contribute greatly to the strength. However, the alloy carbide formed during the γ/α transformation and also on dislocations in the ferrite is much finer in scale, and so would be expected to have a greater influence on the mechanical properties.

It is possible to estimate the contribution to strength from precipitation in a similar manner to that described in Section 8.2 for vanadium steels, by comparing the observed yield stress with that calculated from the grain size, solid solution and basic lattice contributions, and by assigning the difference to the effect of the dispersion. If this is done, a rough figure of 100 MNm^{-2} is obtained for the increment in strength, but this is sensitive to many variables. A more direct indication[61] is obtained from data on a 0.10 pct C, 0.6 pct Mn steel with and without 0.09 pct Cb where the yield stress is plotted against $d^{-1/2}$, d being the average ferrite grain diameter (Fig. 30). When the Cb-containing steel is austenitized at 950°C the plot of yield stress against grain size is almost an extension of the results for the plain carbon steel, reflecting the finer grain sizes achieved by the presence of undissolved particles of CbC, and by the low solution temperature. However as the austenitizing temperature is gradually raised, more CbC is taken into solution to be reprecipitated when the steel is cooled through the γ/α transformation, with a resulting increase in yield stress. The data shows that by using a high austenitizing temperature and comparing steel of the same grain size with and without Cb, an increment of yield stress of over 150 MNm^{-2} is obtained (~10 tsi) which results from a CbC dispersion with a volume fraction of approximately 0.1 pct.

This figure of 0.1 pct volume fraction represents an upper limit available using CbC defined by the solubility of CbC in austenite at the highest practicable solution temperatures (1200–1300°C). Other carbide forming elements provide greater scope because they are more soluble in austenite. The solubility products of the alloy carbides and nitrides familiar in steels given in Fig. 29 show that titanium carbide is more soluble in austenite than columbium carbide, moreover titanium has an advantage in terms of atomic

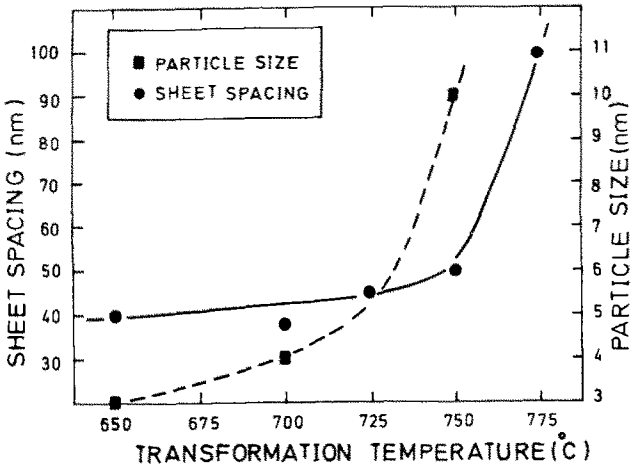

Fig. 31—$\frac{1}{2}$Cr-Mo-V steel isothermally transformed. Dispersion parameters as a function of temperature. (Dunlop)[18]

weight. On the other hand, vanadium carbide is much more soluble than titanium carbide; as mentioned in an earlier section, up to 1.25 pct carbide by volume of VC can be precipitated as a result of the γ/α transformation. Chromium and molybdenum (also tungsten) carbides are still more soluble in austenite, but as the elements are not as strong carbide formers, higher concentrations of alloying element are needed to obtain suitable dispersions. So moving away from micro-alloyed steels to those with higher alloying content and potentially higher strength, it would appear that to utilize strengthening by direct transformation, vanadium and/or titanium would provide the most suitable strengthening carbide dispersions, both by virtue of the achievable volume fraction and their resistance to coarsening during and after transformation. However it should be appreciated that these elements can be added to alloy steels containing for example molybdenum, chromium, and so forth, and despite their lower concentration, still provide the main carbide precipitate. Consequently chromium can be used for oxidation or corrosion resistance, molybdenum for solid solution strengthening, and the dispersion strengthening can still come from those elements such as vanadium and titanium shown to be so effective in micro-alloyed steels. This point is further illustrated in the next section.

10. LOW AND MEDIUM ALLOY STEELS– HIGH TEMPERATURE PROPERTIES

Apart from micro-alloyed steels which are brought to their full strength level by controlled rolling and direct transformation, there are numerous low alloy and medium alloy steels where the possibility of one stage heat treatments exists. For reasons made clear earlier, these are likely to be steels with V, Mo or Ti as elements which provide the carbide dispersion. For example, Dunlop and the author[63] have carried out an extensive study of a $\frac{1}{2}$Cr-$\frac{1}{2}$Mo-$\frac{1}{4}$V-0.1C steel which is a commercial creep resisting alloy used, for example, in the manufacture of steam turbines. It was first confirmed that over the range 650–800°C the transformation from austenite leads to dispersion strengthened ferrite, while in the range 350–650°C the bainite reaction predominates. The ferrite reaction product contained mostly a banded dispersion of VC, but the last region to transform frequently exhibited a fine fibrous form of VC. The dispersion parameters were determined as a function of transformation temperature in the range 650–775°C (Fig. 31) for the interphase precipitation which was shown to be VC.

A comparison of the hardness of the structure, produced by isothermal transformation for 15 minutes at 700°C, *viz.* ferrite, was made with

a) bainite formed in 5 minutes at 500°C

b) martensite formed on oil quenching.

To make a reasonable comparison, all specimens after treatment were subsequently aged at 700°C and the hardness measured. Fig. 32 plots the changes in hardness of the three types of specimen; in the long term the differences in hardness which largely reflect the state of the carbide dispersion are rather small, so it is clear that comparable structures can arise *via* the three routes. However in the case of

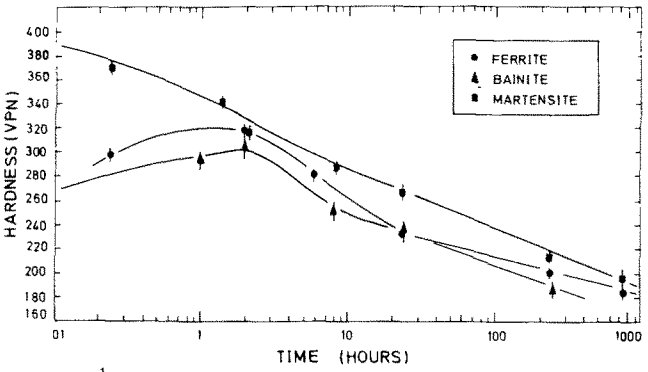

Fig. 32—$\frac{1}{2}$Cr-Mo-V steel: hardness of different starting microstructures after aging at 700°C. (Dunlop)[48]

the latter two treatments a cementite dispersion has to be replaced by the finer VC dispersion during aging. This accounts for the maximum in the hardness curve in the case of the bainitic specimens.

Under practical conditions when this steel is used in creep resistant applications, particularly in thick sections, mixed microstructures are very common, *i.e.* the microstructure is a mixture of ferrite, bainite and tempered martensite so it is difficult to determine the optimum type of structure let alone achieve it under normal industrial conditions. Dunlop[18] has examined under laboratory conditions at 550°C the creep properties of the several "basic" microstructures and made the following conclusions:

1) Primary creep is less extensive in tempered bainitic and martensitic structures than in ferrite, probably because of the much lower dislocation density in the latter structure.

2) The creep strength is markedly increased by raising the austenitizing temperature to allow more VC to dissolve in austenite, then to reprecipitate during subsequent heat treatment.

3) The ferrite produced by isothermal transformation at 700°C can give improved creep rupture life over standard commercial treatments.

The assessment of creep resistant alloys involves many complicated factors and different characteristics are required as the application varies. However the work which has been done so far on dispersion strengthened ferrite formed directly from austenite, indicates that the structures which result have useful high temperature properties, in particular creep rupture life can be improved over alternative structures.

CONCLUSION

I have attempted to show that the addition of alloying elements, particularly those which are strong carbide formers, to steels has some profound effects on the transformation of austenite at high temperatures. In plain carbon steels at these temperatures the relevant phases are ferrite, cementite and pearlite, however in many alloy steels the formation of cementite and pearlite is suppressed, and the alloy carbides adopt different morphologies frequently on a much finer scale than those of the classical phases. It now seems clear that these alloy carbides grow in close association with the ferrite, and as a result their mor-

phology is determined by the mode of growth of the ferrite in austenite during the phase transformation. The general principles underlying the formation of these alloy carbide dispersion strengthened ferrites are gradually being determined, and the way seems clear to a further exploitation of their interesting mechanical properties.

Already micro-alloyed steels make use of dispersion strengthened ferrite additional to grain size strengthening, but it is abundantly clear that a whole range of low and medium alloy steels can exhibit similar (and stronger) structures, although the morphologies are frequently complex. Alloy ferrites formed by direct transformation of austenite are also worthy of examination for use at elevated temperatures, because the very fine alloy carbide dispersions can be very stable and thus possess good creep properties.

ACKNOWLEDGMENTS

I gratefully acknowledge the many contributions made to this work by research fellows and students in the Alloy Steels Research Group at the University of Cambridge. Their work has been specifically referred to in the text, but I would like particularly to thank Dr. D. V. Edmonds for reading the manuscript and for many helpful discussions. Mr. S. D. Charter and Mr. B. Barber rendered valuable assistance in the preparation of diagrams and photographs. I wish to thank the Science Research Council, The British Steel Corporation and the Royal Armament Research Establishment for their continued support.

REFERENCES

1. R F. Mehl and W. C. Hagel *Prog. Met Phys*, 1956, vol. 6, p 74.
2. C. S. Smith *Trans. ASM*, 1953, vol. 45, p. 533
3. R F. Mehl, C S. Barrett, and D. W Smith *Trans. AIME*, 1933, vol. 105, p 215.
4. Y. C. Liu, H I. Aaronson, K. R Kinsman, and M G Hall: *Met Trans*, 1972, vol. 3, p. 1319.
5. C. A. Dubé, H. I. Aaronson, and R. F. Mehl: *Rev Met*, 1958, vol. 55, p 201
6. H. I Aaronson· *Decomposition of Austenite by Diffusional Processes*, p 387 *ff*., Interscience Publishers, New York, 1962.
7. M. Hillert· *Decomposition of Austenite by Diffusional Processes*, p. 197 *ff*., Interscience Publishers, New York, 1962.
8. K. R. Kinsman and H. I. Aaronson *Met. Trans*, 1973, vol. 4, p. 959.
9. H. I. Aaronson, C. Laird, and K. R Kinsman· *Phase Transformations*, ASM 1970, p. 313 *ff*
10. J. V Bee Ph.D. Dissertation, University of Cambridge, 1974.
11. R. J. Dippenaar and R. W. K. Honeycombe: *Proc. Roy. Soc.*, 1973, vol A333, p. 455
12. R. I. Entin *Decomposition of Austenite by Diffusional Processes*, p. 295, Interscience Publishers, New York, 1962
13. M. Mannerkoski. *Acta. Polytech. Scand.*, 1964, Ch. 26.
14. K. Campbell. Ph.D. Dissertation, University of Cambridge, 1971.
15. V. K. Bungardt, E Kunze, and E. Korn *Arch. Eisenhutten.*, 1958, vol 29, p. 193
16. F. G. Berry and R. W K Honeycombe *Met Trans.*, 1970, vol. 1, p. 3279.
17. D. V Edmonds and R. W. K. Honeycombe *J. Iron Steel Inst*, 1973, vol. 211, p. 209.
18. A. T Davenport, F G Berry, and R. W. K. Honeycombe: *Met. Sci J.*, 1968, vol. 2, p. 104.
19. J M Gray and R. B S. Yeo· *Trans. ASM.*, 1968, vol 61, p. 255.
20. S. Freeman *The Effect of Second Phase Particles on the Mechanical Properties of Steel*, ISI London, 1971, p 152.
21. A. T. Davenport and R. W K Honeycombe· *Proc Roy. Soc.*, 1971, vol. 322, p. 191.
22. C. J. Tillman and D. V. Edmonds *Metals Tech.*, 1974, vol. 1, p. 456.
23. W. B Morrison and J. H Woodhead: *J. Iron Steel Inst*, 1963, vol. 201, p. 43.
24. W. B. Morrison *J. Iron Steel Inst.*, 1963, vol 201, p. 317.
25. W. C. Leslie *The Relation Between Structure and Mechanical Properties of Metals*, NPL Conference 1963, p. 337, HMSO, London.
26. J M Gray, D. Webster, and J H Woodhead. *J. Iron Steel Inst*, 1965, vol. 203, p. 812
27. M. Tanino, I. Nishida, I. Ooka, and K Yoshikawa: *Proc. Symp. on Micro-Metallurgy*, Jamshedpur, India, 1965.
28. M. Tanino and K. Aoki *Trans Iron Steel Inst. Japan*, 1968, vol. 8, p 337
29. A. D; Batte and R. W. K. Honeycombe *J. Iron Steel Inst.*, 1973, vol. 211, p. 284, *Met. Sci. J.*, 1973, vol. 7, p. 160.
30. K Campbell and R. W K. Honeycombe *Met. Sci. J.*, 1974, vol. 8, p. 197.
31. V. K. Heikinnen *Acta Met.*, 1973, vol. 21, p 709, *Scandin. J. Met.*, 1974, vol. 3, p 41
32. R G. Baker and J. Nutting *ISI Special Report*, no 64, 1959, p. 1
33. C J. Middleton and D. V. Edmonds *Metallogr*, 1976, in press.
34. T. N. Baker· *Acta Met.*, 1973, vol 21, p 261
35. A. Barbacki and R. W. K Honeycombe *Metallogr.*, 1976, in press.
36. A D Batte: Ph D. Dissertation, University of Cambridge, 1970
37. S. Freeman. Ph.D. Dissertation, University of Cambridge, 1971
38. H J Harding Ph.D Dissertation, University of Sheffield, 1966
39. D J. Dyson, S. R. Keown, D. Raynor, and J. A. Whiteman. *Acta Met*, vol 14, 1966, p. 867
40. D. V Edmonds *J. Iron Steel Inst.*, 1972, vol 210, p 363
41. P. R Hilyman Unpublished work *Met Trans.*, 1973, vol. 4, p. 959.
42. D. V Edmonds Private communication, University of Cambridge.
43. D M Davies and B. Ralph: *J Iron Steel Inst*, 1972, vol 210, p. 262.
44. D M Schwartz and B Ralph *Met. Sci. J.*, 1969, vol. 3, p. 216
45. G L. Dunlop and R. W. K. Honeycombe *Phil. Mag.*, 1975, vol. 32, p. 61.
46. K Kreye *Z Metallk.*, 1970, vol 61, p 108
47. A J Ardell *Acta Met.*, 1972, vol 20, p 601
48. G. L. Dunlop· Ph.D. Dissertation, University of Cambridge, 1974
49. A H. Bowen and G M. Leak *Met. Trans.*, 1970, vol 1, p. 2767.
50. G. L Dunlop and P. J. Turner. *Met Sci*, 1975, vol. 9, p. 370.
51. J S T. Van Aswegen, R. W K Honeycombe, and D. H. Warrington· *Acta Met.*, 1964, vol 12, p. 1.
52. S J. Harris and N. R. Nag: *J. Mater. Sci.*, 1975, vol. 10, p. 1137.
53. Y. E. Smith and C A. Siebert. *Met. Trans.*, 1971, vol 2, p. 1711.
54. V. M. Klestov, R. I. Entin, K. N Sokolov, G Y. A Betin, L. I. Kogan, and N. V. Mikhno: *Fiz. Metal. Metalloved*, 1972, vol. 33, p 973
55. M. M Shteinberg, V. I Filatov, T. I. Shilkova, M A Smirnov, and V. N. Gonshar: *Steel in the USSR*, Oct. 1973, p 872.
56. D J. Walker Ph D. Dissertation, University of Cambridge, 1975
57. T. Gladman, B. Holmes, and I. D. McIvor *The Effect of Second Phase Particles on the Mechanical Properties of Steel*, ISI, 1971, p. 58.
58. F. B Pickering and T. Gladman *ISI Special Report No 81*, 1963, p. 10.
59. T. Gladman· *Proc. Roy. Soc*, 1966, vol. A294, p. 298.
60. D. V. Edmonds *Met. Trans*, 1973, vol. 4, p. 2527.
61. T Gladman, I. D. McIvor, and D. Duheu· *Structure-Property Relationships in Micro-Alloyed Steels*, Microalloying 1975, Washington, Oct. 1975.
62. W B. Morrison and J. A. Chapman. *Controlled Rolling*, Rosenhain Centenary Conf., London, Sept. 1975, *Proc. Roy. Soc.*, in press.
63. G. L Dunlop and R. W. K. Honeycombe *Met. Sci.*, 1976, vol. 10, p. 124.
64. B. Aronsson *Climax Molybdenum Symposium on Steel Strengthening Mechanisms*, 1969, p 77